UNIVERSITY OF CALGARY

Assessment of Bony Damage Using High Resolution Peripheral Quantitative Computed Tomography (HR-pQCT) in Rheumatoid Arthritis

by

Cheryl Carmelle Marie Barnabe

A THESIS

SUBMITTED TO THE FACULTY OF GRADUATE STUDIES

IN PARTIAL FULFILMENT OF THE REQUIREMENTS FOR THE

DEGREE OF MASTER OF SCIENCE

DEPARTMENT OF COMMUNITY HEALTH SCIENCES

CALGARY, ALBERTA

SEPTEMBER, 2011

UNIVERSITY OF
CALGARY

ABSTRACT

Rheumatoid Arthritis (RA) is an inflammatory arthritis characterized by progressive joint damage in the form of joint space narrowing, erosions and secondary osteoarthritis. A growing body of literature advocates for early and aggressive disease treatment to prevent this structural damage. The current method for assessing joint damage, plain radiography, is limited in sensitivity. Advanced technologies are needed to better identify and prognosticate joint damage with acceptable reliability, accessibility, safety and cost. The objective of this thesis project was to test the ability of high-resolution peripheral quantitative computed tomography (HR-pQCT) to measure RA damage. We have demonstrated that HR-pQCT is a sensitive and reliable tool to quantify joint space width, erosion number and location, and periarticular bone density changes related to inflammation. This novel imaging technique shows excellent promise in the evaluation of bony damage in RA.

ACKNOWLEDGEMENTS

Dr. Susan Barr and Dr. Liam Martin have been my personal champions and supporters since my rheumatology training followed by the undertaking of this degree. Working on this project has been incredibly interesting and rewarding, and I really appreciate the opportunity to lead this new area of investigation. You both have always had my best interests at heart, thank you.

I thank Dr. Steven Boyd for allowing me to use his lab, resources and expertise to complete this project. Eva Szabo was critical in providing technical expertise.

Many thanks to the volunteers who consented to participate in this study.

My funding sponsors were the UCBeyond – The Arthritis Society – Canadian Rheumatology Association Rheumatology Post-Graduate Scholarship. The Department of Medicine, University of Calgary, supported my clinical scholar position to enable the completion of my research program. The McCaig Bone and Joint Institute provided my office space. The Boyd lab donated research resources, and is supported by the Canadian Institutes for Health Research and Alberta Innovate – Health Solutions.

Patrick, you have been incredible throughout this journey. Thank you for everything you have done to make this happen.

DEDICATION

Jocelyne and Madeleine, you are amazing daughters.

TABLE OF CONTENTS

LIST OF TABLES

LIST OF FIGURES

LIST OF SYMBOLS, ABBREVIATIONS AND NOMENCLATURE

Anti-CCP	Anti-cyclic citrullinated peptide
BMD	Bone mineral density
BV/TV	Bone Volume to Total Volume Ratio
CHREB	Conjoint Health Research Ethics Board
cm	Centimetre
COBRA	Combinatietherapie Bij Reumatoïde Artritis
CT	Computed Tomography
Ct.BMD	Cortical bone mineral density
Ct.Th	Cortical thickness
CTX-I	Urinary C-terminal crosslinking telopeptide of type-I collagen
CTX-II	Urinary C-terminal crosslinking telopeptide of type-II collagen
DEXA	Dual x-ray absorptiometry
DIP	Distal interphalangeal
DMARDs	Disease Modifying Anti-Rheumatic Drugs
DXR	Digital x-ray radiogrammetry
HR-pQCT	High-resolution peripheral quantitative computed tomography
IL-1β	Interleukin-1-beta
IP	Interphalangeal
K	Kappa
MCP	Metacarpophalangeal

mg HA/cm^3	Milligrams of hydroxyapatite per cubic centimetre
mm	Millimetre
mm^3	Cubic millimetre
MRI	Magnetic Resonance Imaging
MTP	Metatarsophalangeal
OMERACT	Outcome Measures in Rheumatology
OPG	Osteoprotegerin
OSCAR	Osteoclast-associated receptor
PIP	Proximal interphalangeal
Pr(a)	Percent agreement
Pr(e)	Probability of random agreement
RA	Rheumatoid Arthritis
RAMRIS	Rheumatoid Arthritis Magnetic Resonance Imaging Score
RANK	Receptor activator of nuclear factor kappa-B
RANKL	Receptor activator of nuclear factor kappa-B ligand
ROC	Receiver Operating Characteristic Curve
SD	Standard Deviation
Tb.BMD	Trabecular bone mineral density
Tb.N	Trabecular number
Tb.Sp	Trabecular separation
Tb.Th	Trabecular thickness
TNFα	Tumor necrosis factor-alpha
vdHSS	Van der Heijde/Sharp score
µm	Micrometre

μSv	Microsievert

CHAPTER ONE: An Introduction to Rheumatoid Arthritis

1.1 Clinical Presentation

Rheumatoid Arthritis (RA) is a chronic autoimmune condition characterized by inflammation of the synovium of the small joints of the hands, wrists and feet. Local symptoms at these joints include pain, swelling and stiffness. Systemic constitutional symptoms, such as low grade fever and fatigue, and extra-articular features, such as rheumatoid nodules and sicca symptoms, may be present (1). The diagnosis of RA is based on the persistence of clinical symptoms and signs, with additional confirmatory information from autoantibody profiles and diagnostic imaging findings. RA is more common in females, and affects up to 1.1% of the general population (2, 3).

1.2 Pathogenesis of Rheumatoid Arthritis and the Effect of Inflammation on Bone

Pathophysiologic mechanisms responsible for the initiation and progression of RA continue to be investigated. It is currently believed that a variety of environmental exposures, such as smoking or microbial elements, may lead to the creation of pathogenic autoantibodies in a genetically predisposed individual. Resulting abnormalities in immune system signaling and an imbalance between suppressive and proinflammatory mediators lead to an attack on joints lined with synovium (4) (Figure 1.1). The synovium becomes overgrown (termed pannus) under the influence

of interleukin-1β (IL-1β), which also mediates local bone demineralization and loss (osteopenia) (5). The synovium then becomes the principal source of cytokines and proteinases that mediate cartilage damage (6) as well as the site of accumulation and differentiation of osteoclast precursors that result in focal damage to bone (7).

Cartilage damage in rheumatoid arthritis occurs at the cartilage-pannus junction (6). This damage is initiated by a number of immune cell interactions occurring in the synovium, including those between T and B lymphocytes, monocytes/macrophages, and dendritic cells. Matrix metalloproteinases, a group of enzymes which act at the cartilage surface to destroy the joint matrix, are upregulated by pro-inflammatory cytokines IL-1β and tumor necrosis factor-α (TNFα) (5). Chemokines, nitric oxide and prostaglandins further contribute to the pro-inflammatory cascade (6).

Osteoclasts, which have differentiated from mononuclear cells under the influence of TNFα, osteoclast-associated receptor (OSCAR), and interactions between synovial fibroblast-like cells and activated TH1 and TH17 cells, are the main cells responsible for erosion development (7). These cells remove calcium from bone and thus degrade the bone matrix, resulting in an erosion. Typically, erosions are seen at sites where there is no overlying cartilage protection and the pannus has physically invaded either cortical or subchondral bone (8).

Periarticular osteopenia is thought to be a paracrine effect of the inflammatory process resulting from abnormal signaling of the receptor activator of nuclear factor

kappa-B ligand (RANKL), receptor activator of nuclear factor kappa-B (RANK), and the osteoprotegerin (OPG) system, with a negative net effect on local bone mass (7). However, advanced diagnostic imaging has demonstrated substantial decreases in the number of trabeculae along the metaphyses of bones near inflamed joints, suggesting that periarticular bone demineralization is also likely related to physical links between the synovial cavity and the bone marrow, either through cortical penetration of inflammatory tissue through erosions or alternatively by small cortical bone channels (7).

Figure 1.1 Normal and Rheumatoid Arthritis Joint Structure

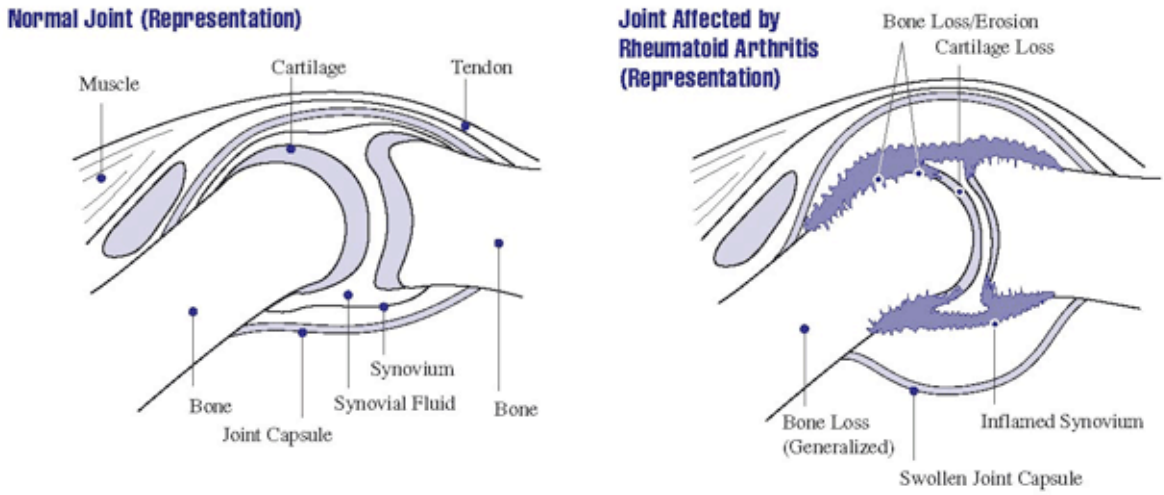

This image is a work of the National Institutes of Health, part of the United States Department of Health and Human Services. As a work of the U.S. Federal Government, the image is in the public domain. Permission PD-USGOV-HHS-NIH.

1.3 Consequences of Rheumatoid Arthritis

Those affected with RA are at risk for local joint damage, as well as systemic morbidity and mortality. Uncontrolled inflammation leads to progressive joint damage, characterized by narrowing, bone erosions, and secondary osteoarthritis (9). This joint damage is strongly associated with disability and reduced quality of life (10-13). Independent of disease activity over time, patients with RA are at increased risk of cardiovascular disease (14) and premature mortality (15). There are significant direct and indirect economic costs attributable to RA (16, 17).

1.4 Rheumatoid Arthritis Treatment

The treatment of RA with disease-modifying antirheumatic drugs (DMARDs) and biologic therapies is directed at achieving symptom improvement, a low disease activity or remission state, and to inhibit joint damage (1). In the absence of adequate therapy, 90% of patients will have erosions and deformities visible by plain radiography within two years of symptom onset (18, 19). Therefore, current treatment recommendations for RA support early and intensive management to reduce structural damage (20). The window of opportunity, where intervention may prevent permanent radiographic damage, may be as short as 12 weeks, as those delayed in seeing a rheumatologist beyond that time point had a 1.3-fold higher rate of progression in their damage score (21). As summarized by Hazes and Luime, approximately 30% of patients initially presenting for care for early arthritis

symptoms of less than 1 year will have undifferentiated arthritis not meeting criteria for RA, with only 13-54% going on to have classifiable disease over the next year and 20-60% spontaneously remitting (22). However, it is not always possible to reliably predict which patients with early symptoms will have self-limited or other forms of mild arthritis as opposed to severe, erosive RA. Thus, the benefits of early intervention need to be weighed against the risks of treatment in those who may not necessarily have a destructive and progressive disease course (23, 24).

Given these considerations, current rheumatology practice and research has placed great emphasis on the early identification and prognostication of RA (25). Screening questionnaires have been developed and validated to identify which individuals with joint symptoms are those most likely to have early RA (26). Dedicated clinics have been created to ensure that patients with inflammatory arthritis receive priority assessment and treatment by specialists (27). Clinical prediction rules have been developed to aid rheumatologists in decision making for patients with undifferentiated arthritis who may evolve into RA, and therefore benefit from early aggressive treatment as opposed to symptomatic treatment and observation (28). Advanced biomarker analysis with highly sensitive and specific autoantibodies may identify those most likely to have aggressive RA with a propensity to progressive joint damage (29).

Another biomarker is diagnostic imaging, in particular highly sensitive imaging techniques (30). Modalities of magnetic resonance imaging (MRI) (31-35), ultrasound (36) and digital x-ray radiogrammetry (DXR) (37-39) have been studied to determine

their ability to identify early RA damage. However, these techniques have limitations with respect to cost, safety, and applicability for widespread clinical use outside of research and specialty centres, such that alternative techniques are being sought to address this need (23). These techniques are described in greater detail in Chapter Two.

CHAPTER TWO: Structural Joint Damage in Rheumatoid Arthritis: Prognostication, Identification and Measurement

2.1 Prognostication of Joint Damage in Rheumatoid Arthritis

Structural joint damage in RA results in functional disability and reduced quality of life. Early identification of RA allows the opportunity to introduce treatment that can slow or inhibit radiographic damage. Particular clinical, laboratory and imaging features characterize patients with RA who are at the highest risk of developing structural damage, and are summarized in the following section. Although it may seem that there are many risk factors that predict a patient's disease course, it is estimated that 20-50% of the variation in joint damage between individuals remains unexplained (40, 41).

2.1.1 Clinical Risk Factors

Patients at the highest risk for developing joint damage include females (42) and patients with rheumatoid nodules (43). Symptom duration prior to diagnosis and treatment (43-45), baseline level of health (46), the number of swollen joints at presentation, and involvement of particular joints are also factors that predict structural damage over time (44, 45, 47). Cumulative disease activity is directly linked to radiographic outcomes (48). More recently, low body mass index (49-51) and low

bone density at disease onset (52) have also been shown to be risk factors for joint damage.

2.1.2 Laboratory Markers

The presence of rheumatoid factor, anti-cyclic citrullinated peptide, shared epitope and an elevated acute phase response are the serological features of aggressive disease (40). A newly identified association for radiologic damage has been described in those with elevated markers of bone turnover such as urinary C-terminal crosslinking telopeptide of type-I and type-II collagen (urinary CTX-I and CTX-II) (53) and beta-C-telopeptide (beta-CTx) (54).

2.1.3 Diagnostic Imaging

Early radiographic evidence of erosions is a marker for aggressive disease (40). For example, analysis of x-rays from the Combinatietherapie Bij Reumatoïde Artritis (COBRA) study showed that the presence of baseline damage in a joint doubled the risk for damage progression in that same joint (41). Other groups have also identified that baseline damage is a predictor of the severity of joint damage over time (43, 46, 55). Periarticular osteopenia, as measured by DXR and as an indicator of severe inflammation, is also identified as a risk factor for joint damage (56). This evidence further supports the concept of early identification of erosive disease in order to intervene aggressively to prevent further damage from occurring.

2.2 Imaging Techniques

Diagnostic imaging allows visualization of inflammation, bony changes, and damage that cannot be determined by clinical examination. A variety of diagnostic imaging techniques exist, each with their own particular advantages and disadvantages for use and interpretation in clinical practice.

2.2.1 Plain radiography, or X-Ray

This is the current gold standard for imaging in RA. X-ray is easily accessible, and rheumatologists are familiar with its interpretation. The technical limitations of x-ray include variations in joint positioning, film exposure, film resolution and reader interpretation (57, 58). X-ray is insensitive in RA and only demonstrates late features of damage (59). It provides a two-dimensional assessment of bone and cannot visualize synovitis or specific soft tissue involvement. These limitations are the stimulus to apply other imaging modalities in RA, including MRI, ultrasound and computed tomography (CT) (60).

2.2.2 Magnetic Resonance Imaging (MRI)

The advantages of MRI technology are related to its multiplanar capability, allowing complete imaging of the joint. MRI also permits assessment of surrounding soft tissues, the synovium and synovial fluid, and can quantify inflammation if contrast is used (61). However, MRI is poor at visualizing bone (62). An MRI image is

created by the presence of mobile protons in tissue producing a signal. Because cortical bone has almost no water, the determination of the joint and erosion margins is dependent on signal voids silhouetted against signal-emitting bone marrow and periosseous tissues. This leads to an overestimation of erosion size, and soft-tissue signal may be misinterpreted as erosive changes. Other disadvantages of MRI include limited availability, cost, and that expert readers are required to correctly interpret the results (63). MRI findings consistent with inflammatory arthritis have been demonstrated in healthy controls (64), and false positive determinations by inexperienced readers without clinical context could result in unnecessary referrals and/or treatment. Finally, if a peripheral MRI machine is not available, scans would occur in the closed magnet, and patients with claustrophobia, morbid obesity and implanted metallic devices could not be scanned.

2.2.3 Ultrasound

There is great interest in Europe and Canada in the use of ultrasound in RA assessment. Ultrasound allows detection of joint effusions, surrounding soft tissue involvement, and erosions, while power Doppler signal identifies the increased tissue vascularity of inflamed tissues (65). Ultrasound can be performed in the examination room and is of low risk to the patient. The disadvantages of this technology include access to an ultrasound machine and appropriate probes for different joints, the

operator dependency of the technique, poor bone visualization, and limitations on views of certain joints (65).

2.2.4 Computed Tomography (CT)

CT is the best modality to assess cortical bone erosions and joint space width (62). Both CT and x-ray depend on differences in attenuation of the x-ray beam by different tissue densities to produce an image. Cortical bone is very dense due to mineralization, and there is a clear delineation between bone and soft tissue. This makes it very easy to determine the location of joint and erosion margins. Like MRI, CT has multiplanar capabilities, and multidetector CT technology has proven to be superior in the detection of erosions relative to MRI and x-ray in comparative studies (62, 66). Application of CT technology alone in RA damage assessment has been limited to one clinical trial of adalimumab, a biologic drug used to treat RA (67). CT has not been widely studied in RA yet, related to the accessibility of scanners, and also that the most recent research in RA imaging has focused on soft tissue abnormalities. There is also heightened concern of the risk of repeated radiation exposure and the theoretical risk of associated side effects in the long term. This risk is minimized when a focal extremity or region of interest is imaged.

2.3 Measurement of RA Damage

Erosions and joint space narrowing are relatively objective permanent features of joint damage that can be assessed reproducibly and are the basis for radiographic damage scoring systems (57). Periarticular osteopenia, however, is a subjective radiographic feature of RA that is not included in formal scoring systems (63). Semiquantitative scoring systems are widely used in clinical trials, whereas quantitative measures of joint damage are mainly applied in the research setting.

2.3.1 Semiquantitative Methods – Plain Radiography

Semiquantitative methods of determining RA bony damage include two well recognized scores, the Larsen score (68) and the Sharp score (69), and their variations. The Larsen score is an ordinal score assigned based on comparison of the patient's radiograph and a set of reference films, with an overall grade assigned to each joint for the quantity of erosions present and joint space narrowing (68). The Sharp score is an ordinal score with individual values assigned for joint space narrowing and erosions (69). A modification of the Sharp score by van der Heijde is currently the preferred method for detailing joint damage in clinical trials (70) (Table 2.1). The van der Heijde/Sharp score (vdHSS) allows separate scores to be assigned per joint for both width and percentage of joint space destroyed by erosions (70).

Table 2.1 Joint Space Narrowing and Erosion Scores by the van der Heijde/Sharp Method

Score	Joint Space Narrowing	Erosions
0	Normal	None
1	Focal or Doubtful	Discrete erosion (1 point for each to maximum of five)
2	Generalized, > 50% of the original joint space left	Larger erosion, does not extend over the imaginary middle of the bone
3	Generalized, < 50% of the original joint space left or subluxation	Larger erosion, extends over the imaginary middle of the bone
4	Bony ankylosis or complete luxation	No description
5	Not applicable	Complete involvement or collapse of the bone

2.3.2 Quantitative Methods: Joint Space Width

Direct measures of joint space width at the midpoint of the joint have been obtained with plain radiograph (71). Methods to define the reference points for the measurement vary between investigators, thus the actual numerical value obtained is felt to be less important than obtaining the within-joint change over time (72, 73).

A number of investigators have used software programs for digital x-ray films to approximate joint margins that are damaged or obscured. Automated algorithms can identify joint space locations and orientation by determining changes in gray scale intensity. The joint space width is taken as the average distance between the delineated margins in a central measurement region (74-76).

Sharp et al manually identified the joint margins by placing markers on the edges of the joints using a plug-in application to an imaging program, with automatic calculation of the minimum and mean joint space once the image was smoothed by a polynomial curve applied along sample points (77). Two groups have manually approximated the joint location and medial axes of phalanges but the actual joint margins were detected by changes in pixel intensity and gradients (78-82).

To date, no methods for determining joint space width with CT have been published. Outcome Measures in Rheumatology (OMERACT), a consensus group developing a scoring system for RA using MRI, eliminated joint space width from its score early on in the development of the tool. There was lack of reliability in reader agreement and difficulty in measuring joint space in the small joints of the hands and wrists (83). MRI technology has improved in the interim, renewing the interest in studying this parameter. Recently, definitions for joint space narrowing of the wrist have been proposed (84).

Joint space width measurements have also been determined using DXR, a technology used in measuring bone mineral density in the hand (Pronosco X-Posure System version 2.0; Sectra Pronosco A/S, Denmark) (37, 38). Using a software

program, the reader determines a rectangular region of interest around the joint. Over a 1.5 centimetre (cm) path, the average joint space measurement over a 0.8 cm segment is calculated.

2.3.3 Quantitative Methods: Erosion Volume

There is controversy in the assessment of erosion volume. Some investigators believe that estimates of volume are erroneous since in most cases there is no baseline reference for the periosteal contour prior to erosion development, such that it is not possible to be sure where the original margin actually was. Additionally, the ability to calculate erosion volume by x-ray is limited by the difficulty in determining the edge of an active erosion since the normal bone density gradually fades into the background soft tissue density, in contrast to a 'healed' or corticated mature erosion (58). As well, x-ray images are only two dimensional, as compared to the three-dimensional aspects of a volume measurement.

Other investigators believe that estimating erosion volume is valid. Higgs et al applied templates of circles and semicircles of known size in comparison to the x-ray images (71). Buckland-Wright et al used microfocal radiography to magnify the images, and traced the erosion boundaries with a wax pencil to calculate the dimensions (85). Sharp et al used software to delineate a region of interest around an erosion (77). The mean density per cubic millimetre of bone was calculated for that region of interest, and compared to that of an anatomically similar site in an adjacent uninvolved bone. The quantitative erosion volume using this technique was more

sensitive to treatment effects than ordinal scoring methods. An interesting technique used automated methods to delineate the bone contours, with classification of either a healthy bone contour or abnormal contour based on texture features comprising gradients and gray value deviation (76).

Duryea et al has used a simulation study and in vivo validation to determine carpal bone erosion volume on CT by comparing local volume differences (86). Reliability of the results improved when a local region of interest was delineated as opposed to considering the whole area of study. There was difficulty, however, locating erosions that were parallel to the axial plane due to problems with segmentation at that location. Moller Dohn et al used CT images reconstructed in both axial and coronal planes in an adalimumab clinical trial to demonstrate radiologic stability and even regression of erosions after 6 and 12 months of treatment (67).

MRI evaluation of erosions in the wrist or metacarpophalangeal (MCP) joints is guided by OMERACT's scoring system named RAMRIS, with ordinal scoring based on the proportion of eroded bone compared to assessed bone volume (87). Erosions were defined as sharply marginated bone lesions, with correct juxtaarticular localization and typical signal characteristics visible in two planes with a cortical break seen in at least one plane (88). Bird et al used imaging software that calculates erosion volume once the erosion is manually outlined, with visualization one centimetre proximally and distally from the joint margin for the MCPs (89, 90).

2.3.4 Quantitative Methods: Periarticular Osteopenia

Periarticular bone density has not been quantified with the conventional imaging techniques of x-ray, CT nor MRI, but DXR has been used (39, 91). With this method, an active shape model and computer algorithm automatically defines regions of interest around the narrowest parts of the 2nd, 3rd and 4th metacarpals. The bone density is calculated as volume per area, corrected for estimated porosity and surface area analyzed.

Dual x-ray absorptiometry (DEXA) measurements in the hands have been obtained for multiple locations, including the whole hand, the distal 1.5 cm of the 2nd through 5th metacarpal bones of the non-dominant hand (92, 93), subchondral regions or the whole metacarpal (94), or directly over or on either side of the distal interphalangeal joints (DIPs), proximal interphalangeal joints (PIPs), MCPs or mid metacarpal region (95). Better precision was obtained when density was measured directly over the joint. This technique does not measure other features of joint damage.

2.4 Selection of Joints for Assessment

RA is a symmetrical polyarthritis affecting the small joints of the hands (PIPs and MCPs) and feet (metatarsophalangeal (MTP) joints) as well as the wrists (Figure 2.1). Damage is more pronounced in the dominant hand, with a high likelihood of PIP and MCP involvement (96-98). In x-ray assessment, measurement of four PIPs, four

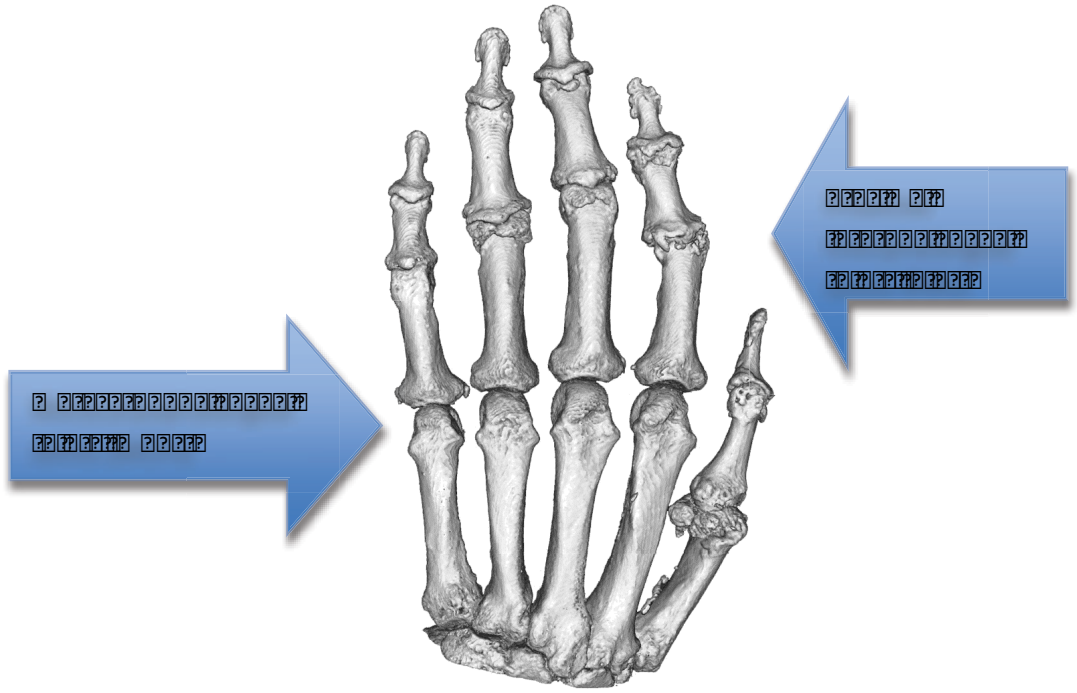

CHAPTER THREE: High-Resolution Peripheral Quantitative Computed Tomography Technology and its Application in Rheumatoid Arthritis Imaging

3.1 Introduction to High-Resolution Peripheral Quantitative Computed Tomography (HR-pQCT)

HR-pQCT (Scanco Medical AG, Brüttisellen, Switzerland) is a novel peripheral CT instrument capable of accurately and reproducibly imaging bone microstructure at a nominal isotropic voxel dimension of 82 micrometres (μm), compared to current clinical CTs that typically provide 400 μm in-plane resolution (99-102). Precise measures of three-dimensional microstructural morphometric parameters and volumetric density of the cortical and trabecular components of bone are possible, with minimal radiation exposure (<3 microsieverts (μSv) per scan, compared to 100,000 μSv for a standard plain radiograph) (103). Therefore, HR-pQCT has the potential to identify and quantify early microstructural bone quality changes before permanent bone damage has occurred. Additionally, non-invasive estimations of bone composition and biomechanical properties are possible using finite element analysis software (99, 104).

3.1.1 Image Acquisition

The patient's limb is immobilized in a carbon fiber cast and is placed within the HR-pQCT instrument. The hardware of the scanner consists of an x-ray source and

detector unit which interfaces with a high-resolution motorized gantry. An initial scanning x-ray is performed to ensure that the area of interest is visualized. The x-ray source and detector moves along the z-axis of the scanner and rotates across 180 degrees to acquire the images required for CT reconstruction. One scan, or stack, captures 110 slices, or 9.02 millimetres (mm) in length.

The procedure for analyzing the obtained images is semi-automated. To start, an approximate contour is drawn around the cortical bone surface. The software then uses an edge detection process to identify the periosteal surfaces of both the proximal and distal bones comprising each joint, proceeding through the 110 slices of a stack. Quality control consists of viewing each individual slice and manually correcting any detection errors from the semi-automated procedure. Images can be viewed in two-dimensional planes and with a three-dimensional reconstruction, which allows rotation of the bone to be viewed from different angles as well as in various planes of cross-section. The software program defines cortical and trabecular bone components separately, allowing quantification of particular features of the bone microarchitecture, termed morphometric indices, which describe the composition of bone (Table 3.1).

Table 3.1 Morphometric Indices and Units of Measure

Index	**Annotation**	**Unit of Measure**
Relative Bone Volume (= Bone Volume/Total Volume)	BV/TV	%
Whole Bone Mineral Density	BMD	Milligrams of hydroxyapatite per cubic centimeter (mg HA/cm^3)
Density of the cortical portion of bone	Ct.BMD	Milligrams of hydroxyapatite per cubic centimeter (mg HA/cm^3)
Density of the trabecular portion of bone	Tb.BMD	Milligrams of hydroxyapatite per cubic centimeter (mg HA/cm^3)
Average cortical thickness	Ct. Th	Millimeters (mm)
Average trabecular thickness	Tb.Th	Millimeters (mm)
Trabecular number	Tb.N	1/millimeter (1/mm)
Trabecular separation	Tb.Sp	Millimetres (mm)

3.1.2 Reproducibility

Prior studies have demonstrated that HR-pQCT image acquisition is highly reproducible, with coefficients of variation of less than 1% for density measures, and a maximum of 5% for biomechanical and morphometric measures (101, 105). Longitudinal assessment over time is possible using slice matching or three-dimensional imaging registration techniques to ensure that the same region is being scanned and analyzed (99).

3.2 HR-pQCT Studies in Rheumatoid Arthritis

The adaptation of HR-pQCT in RA imaging is in its infancy, with only four manuscripts published by two research groups in the last year.

3.2.1 Stach et al (106)*, Finzel et al* (107)*,* (108)

The initial publication of HR-pQCT use in RA came from Stach et al in Germany (106). In their pilot study of 58 patients with RA and 30 healthy controls, they used HR-pQCT to semiquantitatively evaluate bony changes at the 2nd, 3rd and 4th MCP joints and the wrist. These changes included the presence of cortical breaks and their depth, osteophyte formation along the cortical lining, and surface irregularity of the cortex. Models were created to determine if the combination of different bone changes could distinguish RA patients from healthy controls.

Both healthy controls and RA patients were found to have erosions, however erosions greater than 1.9 mm in diameter were highly specific for RA, with the diameter of the cortical break being more important than the depth of the erosion. Osteophytes that were identified correlated with patient age, and not disease status. On three-dimensional images, surface irregularities of the cortical bone were detected, which they concluded represented thinning or fenestration of the bone surface. These were small in area for healthy controls but affected a large part of the bone surface of RA patients. Erosions were particularly common on the radial aspects of the metacarpal heads, and mostly at the 2nd and 3rd MCPs. Osteophytes were mainly found at dorsal and palmar sites.

In a second paper from that group, the shape, size and depth of erosions was compared between RA patients and psoriatic arthritis patients (107). They concluded that psoriatic arthritis erosions were overall smaller in size and depth, with 'omega' or 'tubule' shapes compared to 'U' shaped lesions in RA. There was also a difference in the distribution of the erosions, with RA patients having a strong preponderance for the radial aspect of the metacarpal head, whereas psoriatic arthritis lesions were uniformly distributed. As well, psoriatic arthritis patients had an increased number, extent and size of osteophytes.

The most recent paper from this group compares erosions found by high-resolution ultrasound and HR-pQCT (108). High-resolution ultrasound missed 9.9% of erosions, primarily small erosions at the dorsal sides of MCP joints. Additionally, bony lesions thought to be erosions by ultrasound were actually vascular bone channels at

the palmar sides of the MCP joints and pseudo-erosions created by osteophytes. This error was found in 28.6% of scans.

3.2.2 Fouque-Aubert et al (109)

Fouque-Aubert et al have published on the use of HR-pQCT to assess erosion volume and morphometric indices, and they also supplied reproducibility data (109). They enrolled 36 patients with early RA (all with disease duration < 2 years, mean 1.0 years) with no x-ray erosions, 57 patients with established RA (minimum 3 years duration, mean 8.9 years), and 43 healthy controls. The 2nd and 3rd MCP joints of the right hand were imaged, and they based their analysis on 110 slices at the 2nd MCP and 73 slices at the 3rd MCP.

Erosions were defined as sharply marginated bone lesions with juxta-articular localization and a cortical break in at least two adjacent slices. To calculate the erosion volume, they manually defined a region of interest for each erosion, and used the mean area of the slice, the total number of slices and the slice height in their calculation. Despite the absence of radiographic erosions in the early RA group, 7 patients were found to have erosions at the 2nd MCP and 6 had erosions at the 3rd MCP by HR-pQCT. Additional erosions were also found by HR-pQCT in patients with established RA at the 2nd MCP (n=4 of 14) and at the 3rd MCP (n=6 of 12). Erosion volume was substantially less in the early RA patients (5.3 mm^3 at the 2nd MCP, 4.4

mm^3 at the 3rd MCP) compared to the established RA patients (23.4 mm^3 and 21.5 mm^3, respectively).

RA patients had significantly lower total volumetric BMD at the 2nd MCP (difference 6.2%) and lower trabecular BMD (difference of 7.8% at the 2nd MCP and 5.3% at the 3rd MCP). Trabecular thickness was reduced at the MCP joints in those with RA (difference of 6.5% at the 2nd MCP and 8.4% at the 3rd MCP) relative to control subjects. In this cross-sectional analysis, BMD, trabecular BMD and trabecular thickness negatively correlated with disease activity and inflammatory marker results, but there were no correlations with age, disease duration nor Sharp score, and no difference in parameters depending on anti-cyclic citrullinated peptide status and treatment.

Reproducibility for morphometric indices was high in this study. Coefficients of variance for BMD were 0.7% to 1.8% in established RA and 0.6% to 1.4% in healthy controls. Coefficients of variance for trabecular number, thickness, separation and distribution and cortical thickness were between 3.3 and 12.5% for established RA patients, and 2.9 and 6.3% for healthy subjects.

CHAPTER FOUR: Project Rationale and Objectives

The main objectives of this pilot study were to develop a method for measuring RA joint damage using HR-pQCT and to determine the feasibility of applying this technology in patients with inflammatory arthritis. This is a novel application for HR-pQCT technology, which has previously been used mainly in osteoporosis research. At the time this project was initiated, there was no published literature on the use of HR-pQCT for the assessment of RA joint damage. The research questions that were addressed are summarized below.

4.1 Is it feasible to use HR-pQCT to study small joint damage?

We wanted to develop and standardize a positioning technique that was comfortable for patients with acute and chronic joint disease, while minimizing motion in order to maximize image quality. We noted the time required to scan and analyze joints in order to determine if this imaging technique is practical for patients, clinicians and technicians.

4.2 Can quantitative measures of rheumatoid arthritis damage be obtained using HR-pQCT?

The specific measures we wanted to capture were joint space width and periarticular morphometric indices, and the number and site of erosions. We recruited RA patients with established damage of the MCP and/or PIP joints and age-, sex-, and dominant-hand matched healthy controls in order to assess the ability to acquire these measurements in both diseased and healthy populations. Quantitative measurements in RA imaging could assist in the longitudinal evaluation of treatment adequacy.

4.3 How does HR-pQCT perform relative to standard x-ray in identifying erosions?

X-ray images are two-dimensional, and x-ray is insensitive to early joint damage. Since HR-pQCT provides improved resolution and a three-dimensional view of joint anatomy, we wanted to determine if it is superior to x-ray in identifying erosive damage. This could be important in prognostic studies in patients with early RA or undifferentiated arthritis.

4.4 Can HR-pQCT be used as a diagnostic test for rheumatoid arthritis?

Erosions are considered diagnostic in RA. Therefore, the sensitivity, specificity, predictive values and likelihood ratios of erosion identification by HR-pQCT were calculated given RA or control subject status.

CHAPTER FIVE: Methods

5.1 Study Design

This was a cross-sectional study of subjects with established RA and healthy age-, sex- and dominant-hand matched controls.

5.2 Participants

5.2.1 Major Inclusion Criteria

Fifteen subjects meeting the American College of Rheumatology 1987 Classification Criteria for RA (110) were recruited from the practices of rheumatologists affiliated with the Division of Rheumatology at the University of Calgary. Fifteen age- (within 5 years), sex- and dominant-hand- matched control subjects were identified from the same rheumatology practices where they were assessed and deemed not to have an inflammatory arthritis, or by responding to recruitment posters within the clinic area. Prior to enrollment, digital plain radiographs of the dominant hand performed within the past year as part of clinical care were reviewed by a rheumatologist (Dr. Barnabe) to confirm that joint space narrowing or erosive changes were present at either the PIP or MCP joints for the RA subjects, and that these same joints demonstrated no major abnormalities that might impair interpretation and scoring for the control subjects.

5.2.2 Major Exclusion Criteria

Control subjects with overt evidence of osteoarthritis at the joints of interest or any subjects with prior surgery of the MCP or PIP joints were excluded. Pregnant females were also ineligible.

5.3 Procedures

5.3.1 Questionnaire

RA subjects completed a short questionnaire to provide basic demographic information about their disease. This included their disease duration, autoantibody status, and medication exposures. Formal assessments of disease activity were not included, as this was a cross-sectional study and it would not be possible to account for disease activity or severity accumulated over time in the absence of prospectively collected data.

5.3.2 HR-pQCT Scan

The HR-pQCT scan was performed with the 82 μm XtremeCT (Scanco Medical AG, Brüttisellen, Switzerland). A standard stabilization platform was created to secure the dominant hand, with the MCP and PIP joints extended to a flat position (unless prevented by fixed joint angulation). A scout view x-ray was performed to identify the joints of interest and set the reference line for starting the scan. The 2nd, 3rd and 4th

PIP joints and 2nd, 3rd and 4th MCP joints were scanned together in two sequential stacks, respectively. The other joints (interphalangeal (IP) joint of the thumb, 1st MCP, and 5th PIP and MCP) were each scanned in one stack separately. The total scanning time was under 25 minutes for all ten joints imaged, with a pre-calculated radiation exposure of less than ¼ of a standard chest radiograph.

5.4 HR-pQCT Image Analysis

5.4.1 Contouring and Segmentation

First, individual joints were identified in the scan manually. A simplified version of the automatic contouring algorithm developed by Buie et al (111) was then used to identify the periosteal surfaces of both the proximal and distal bones comprising a joint (Figure 5.1). Each slice was viewed to ensure that the generated contours in the iterations were accurate and correctly identified the bone/soft tissue interface, in particular at the joint margin itself. Subsequently, the mineralized tissue was determined using the manufacturer's standard global thresholding technique and a three-dimensional image was generated (103) (Figure 5.3).

Figure 5.1 Representative Images of the Contouring Process

a) Rough Contours: An approximate contour is drawn around the bones of interest by the analyst.

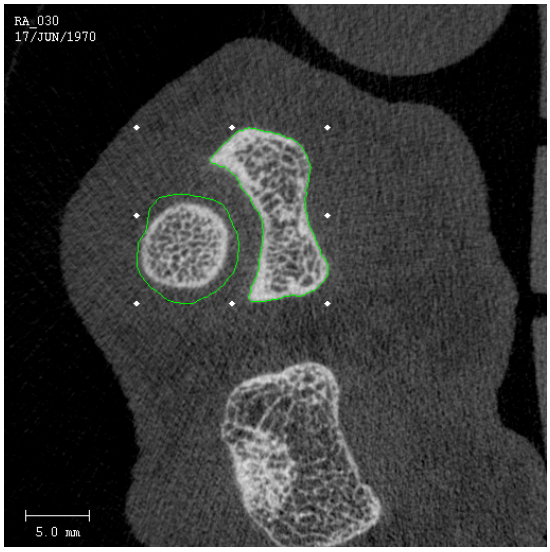

b) Close Contours: The software algorithm automatically detects the largest difference in gray-scale to identify bone from surrounding soft tissues.

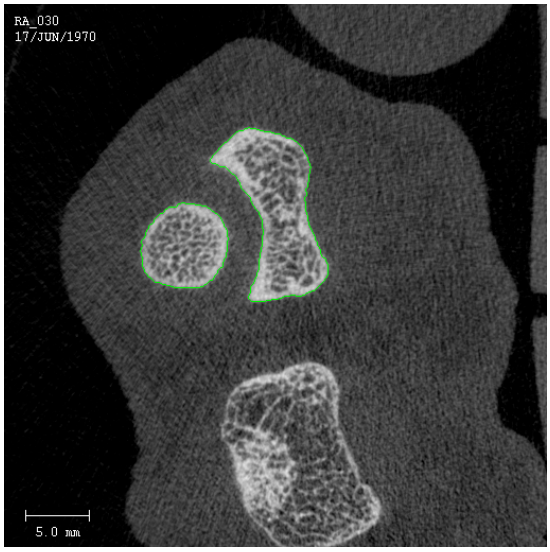

CC

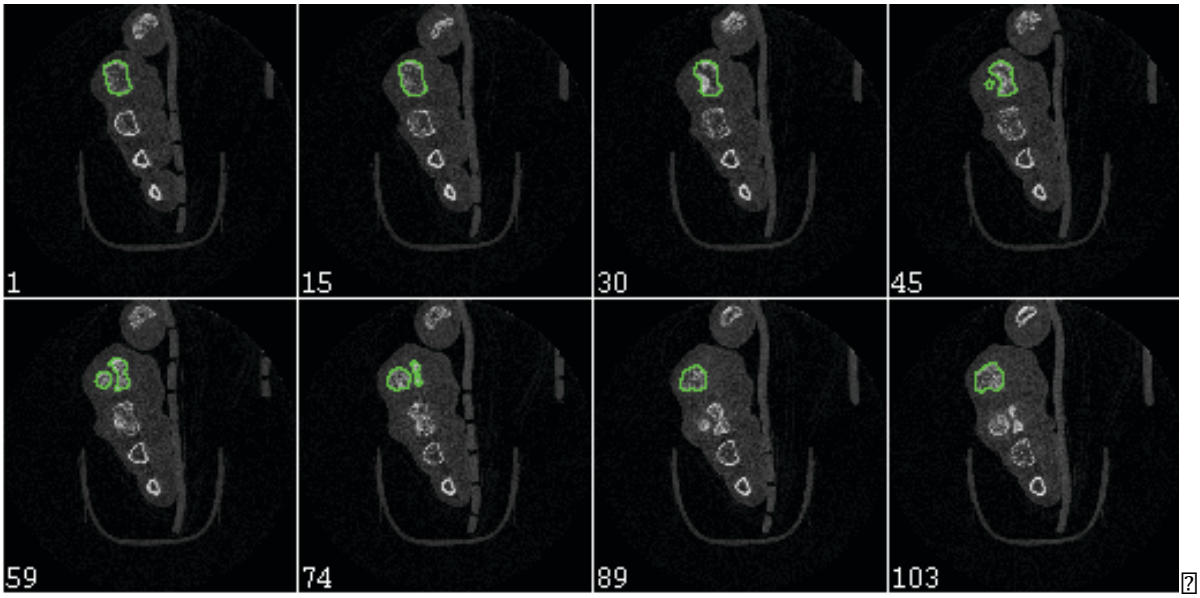

d) Creation of the Three-Dimensional Image: The software program uses the information from the contouring process to render a three-dimensional image of the joint.

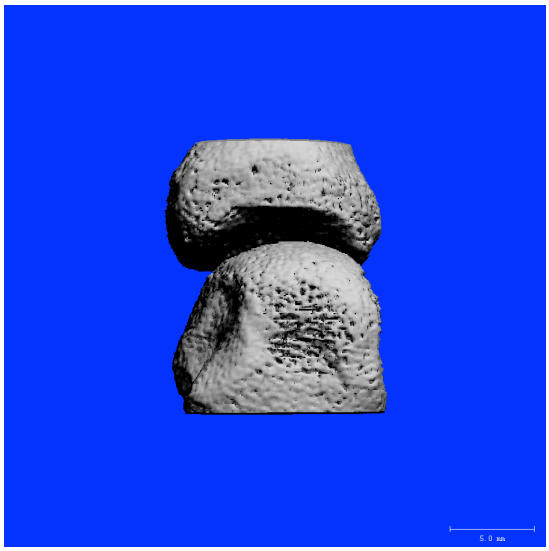

5.4.2 Determination of Joint Space Width

To determine the minimum joint space width, region growing was performed on the three-dimensional representation (Image Processing Language, Scanco Medical, v5.08B). An 82 μm layer was added simultaneously to both proximal and distal bone margins comprising a joint (Figure 5.2). A direct thickness measure of the joint space at the narrowest location was defined as the joint space width measurement (112).

Figure 5.2 Representation of Region Growing. An 82 µm layer is added to both the distal and proximal bone surfaces comprising the joint for each iteration. These layers are added sequentially until one solid object is detected by the software program.

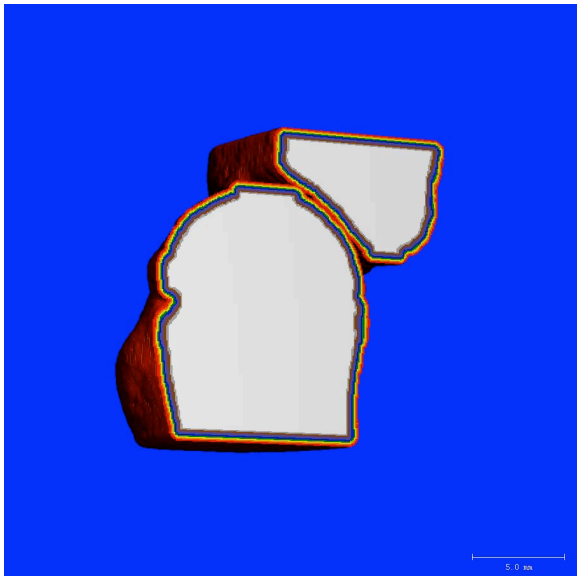

5.4.3 Determination of Morphometric Indices

A region of 60 slices (4.9 mm) from the articular surfaces of each of the metacarpal head and phalangeal base for the 2nd and 3rd MCP joints was used to determine periarticular morphometric indices, for a total region of analysis of 9.84 mm per joint. A fully automated method (dual-threshold segmentation algorithm) was applied to detect the endosteal surface, which is the interface between cortical and trabecular bone (111).

I ngng c i. 1 c 1 i n 1n

Aorhot r t A 1lt r 1lt hs oAsh rmA u ot sc oL ha t rhot rma ns t lt o) A a lt ha (a o 1sRA N7 4a rmh r lh (A /.C% RA oAsRo ot rmal mat r Tl oAot rnj mot hs(lht rnj sA t r) Ar %a Tlh (A /.B% t sR sRA L ha t rhot rma A ot rsA(shot t A)h c so ot 1hAa sR A r t o 1t Aorhot. R Aorhot t r o(t s lt h)h(rmmj t oslt hsr rmo shot z d(A t s Tl oAr rma(rn Aj oAr rmA h rnj i rma A A[rn A t 1 rma A A h r%a oA osRsR Aonha rmat hrs rmot r oa i Arlt eolt s.

Ht : SHF : nH R I : E HR IH R

1 : nH R IC BR R A HRI r Ho HR : R TOT R

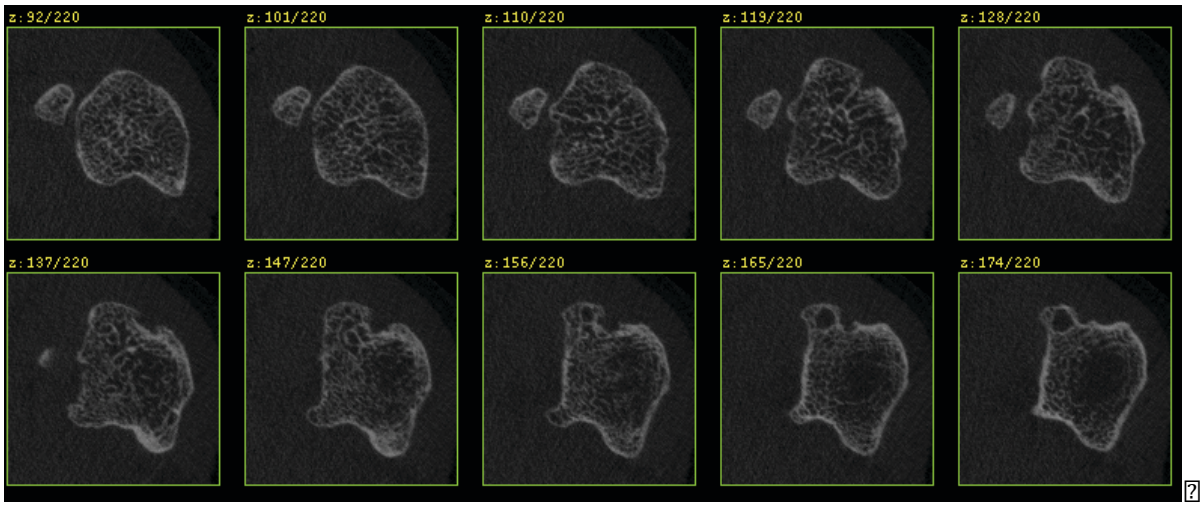

Cα

1 E A HRI R: nH Rd H o HR T R Ht HR T R

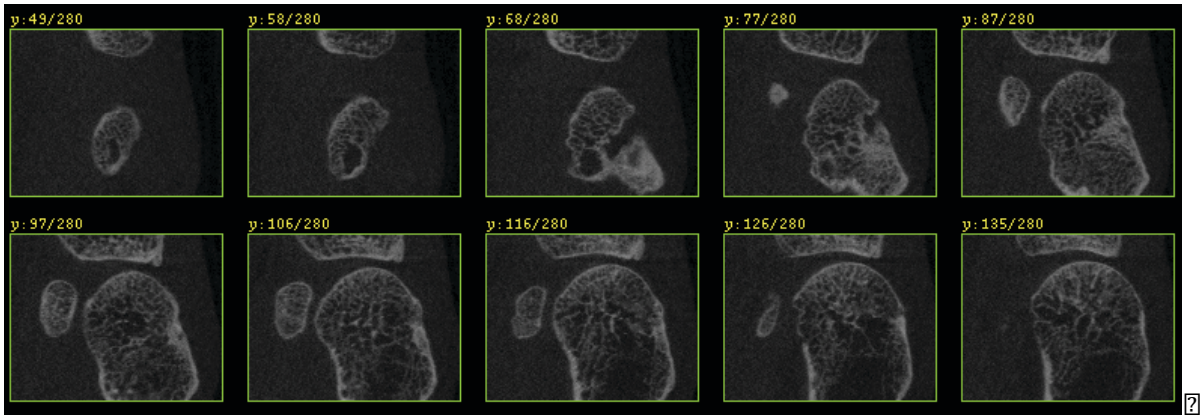

1 E A HRI R: nH Rd H o HR 1: Rnr : n T R

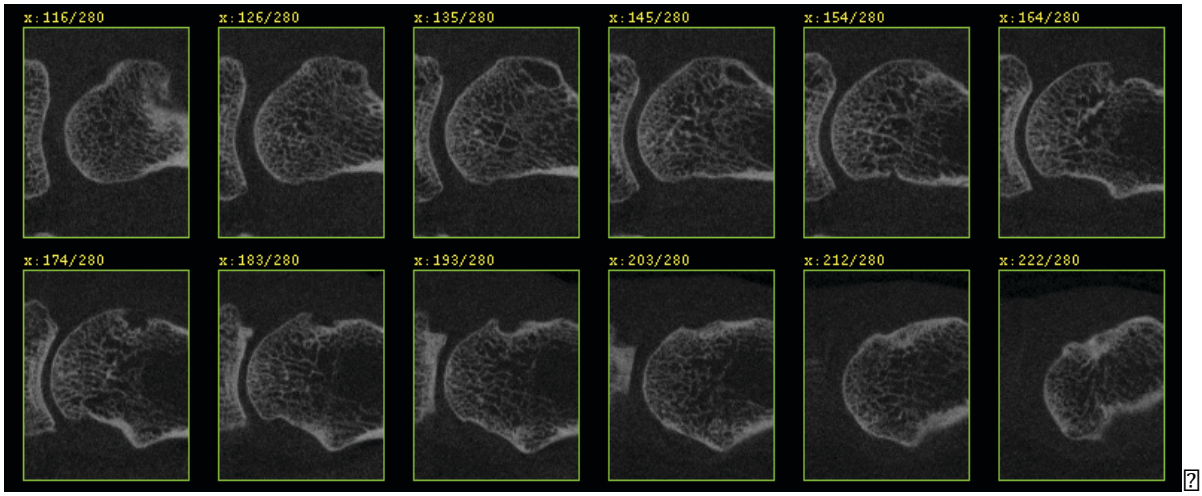

CN

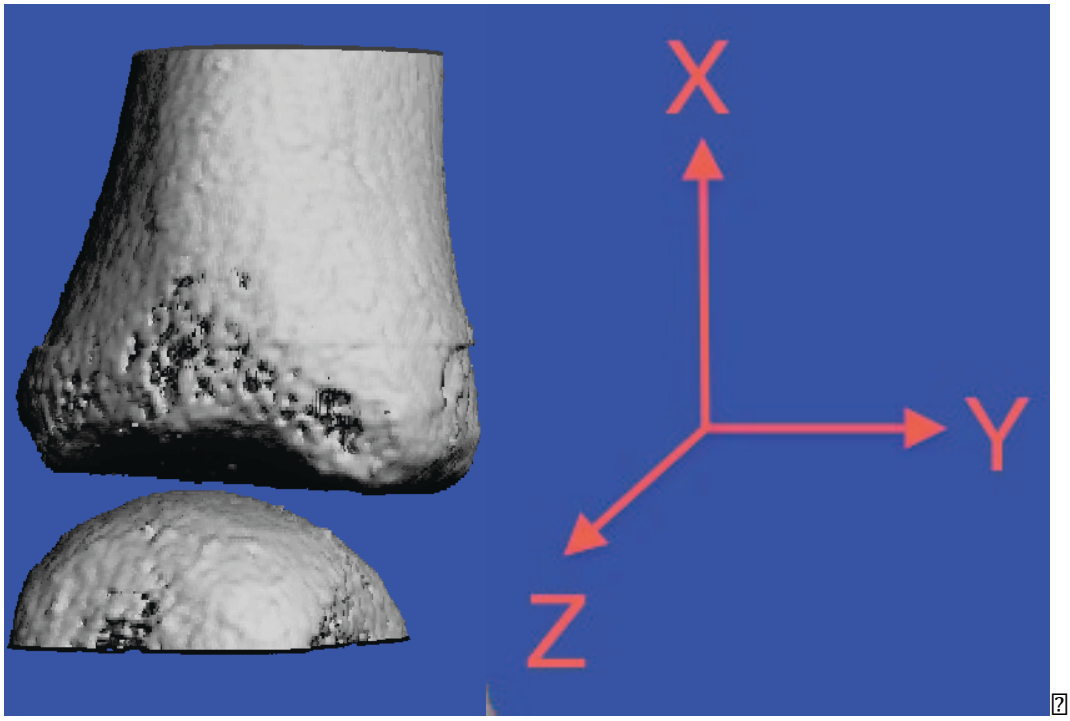

Table 5.1 Image Quality Grades Recommended by the HR-pQCT Manufacturer, Scanco Medical AG

Image Quality Grade	Description
Grade 1	Perfect scans, no motion artifacts visible.
Grade 2	Good scans. Very slight artifacts, horizontal streaks at upper and lower end of radius/tibia just visible.
Grade 3	O.K. scans. Horizontal streaks visible, but cortex still 'fits together'.
Grade 4	Bad scans. Large horizontal streaks, cortex hardly fits together, trabeculae also smeared (little half moons).
Grade 5	Unacceptable scan. Should be excluded.

5.5 Reproducibility

This study did not specifically address the reproducibility of repeat positioning and scanning, but a prior publication has demonstrated that repositioning errors account for less than 1.5% of the variability in measurements (101). Thirty (30) randomly selected images with image quality grades between 1 and 3 were re-contoured to calculate the reproducibility of joint space width and morphometric

indices, and re-scored for erosion count. This second analysis for reproducibility was done blinded to results of the first analysis, and performed at least one month later.

5.6 Radiograph Scoring for Erosions

Two experienced rheumatologists individually viewed and scored the PIP joints and MCP joints for erosions, assigning an erosion score according to the vdHSS as described in Chapter 2 (70).

5.7 Statistical Analysis

5.7.1 Subject Demographics and Comparative Analysis

Subject demographics were summarized descriptively as means or proportions as appropriate. The average erosion count and standard deviation for each joint and all joints overall was calculated for RA and control subjects. We further characterized the location of erosions by proximal or distal bone surface comprising the joint.

Analysis of joint space width and morphometric indices for RA and control subjects occurred within matched sets, defined by age-, sex- and dominant-hand. The mean difference between RA and control subjects within each set was calculated, and the average set difference presented. As this was primarily a feasibility study, we did not power the study to identify differences between groups statistically. However, for normally distributed data, a paired t-test was performed to compare results between

RA and control subjects. For non-normally distributed data, the Wilcoxon signed-rank test was performed.

5.7.2 Reproducibility

To determine the reproducibility of joint space width measurements and morphometric indices, we used the root mean square coefficient of variance (113). The within subject coefficient of variance is calculated by taking the square root of the within subject variance squared, and then dividing by the squared subject mean. Both the within subject variance and mean are divided by two to reflect the two separate readings.

$$\textbf{Within subject coefficient of variance} = \frac{(\sqrt{(x-y)^2})/2}{((x+y)/2)^2}$$

The percent agreement and kappa score (chance corrected proportional agreement) was used to assess the reproducibility of the erosion count (114).

$$\textbf{Percent agreement, Pr(a)} = \frac{\text{Both readers respond in positive + Both readers respond in negative}}{\text{Total number of possible responses}}$$

Probability of random agreement, Pr(e) =

(Probability of positive response reader A)(Probability of positive response reader B)

+

(Probability of negative response reader A)(Probability of negative response reader B)

$$\textbf{Kappa, } \kappa = \frac{Pr(a) - Pr(e)}{1 - Pr(e)}$$

5.7.3 Performance of HR-pQCT Relative to Standard X-Ray

An erosion in a joint was determined to be present on plain radiograph if a vdHSS erosion score of 1 to 5 had been assigned for that joint (70). An erosion was determined to be present on HR-pQCT if any erosion had been scored. The probability of agreement (i.e.concordant and discordant findings) between the two imaging methods was calculated.

5.7.4 HR-pQCT as a Diagnostic Test for Rheumatoid Arthritis

Since erosions are considered diagnostic for RA, we compared the finding of erosions by HR-pQCT to the clinical identification of disease. Various algorithms of erosion findings by HR-pQCT were tested to determine the sensitivity, specificity, predictive values and likelihood ratios in determining clinical RA disease. The optimal

algorithms were determined based on the c-statistic, or area under the curve, for the generated receiver operating characteristic (ROC) curves (115).

$$\textbf{Sensitivity} = \frac{\text{number of true positives}}{\text{number of true positives} + \text{number of false negatives}}$$

$$\textbf{Specificity} = \frac{\text{number of true negatives}}{\text{number of true negatives} + \text{number of false positives}}$$

$$\textbf{Positive Predictive Value} = \frac{\text{number of true positives}}{\text{number of true positives} + \text{number of false positives}}$$

$$\textbf{Negative Predictive Value} = \frac{\text{number of true negatives}}{\text{number of true negatives} + \text{number of false negatives}}$$

$$\textbf{Positive Likelihood Ratio} = \frac{\text{Sensitivity}}{\text{1-Specificity}}$$

$$\textbf{Negative Likelihood Ratio} = \frac{\text{1 – Sensitivity}}{\text{Specificity}}$$

$$\textbf{C-statistic (=area under the ROC curve)} = \frac{\text{Sensitivity + Specificity}}{2}$$

5.8 Ethics

This project was approved by the Conjoint Health Research Ethics Board (CHREB), University of Calgary. CHREB was also supplied with the radiation safety certificate from the University of Calgary.

CHAPTER SIX: Results

6.1 Subject Characteristics

The majority of the included subjects were right-handed females, with an average age of 46 years (Table 6.1). The RA subjects had long-standing disease, the majority were seropositive, and they had been exposed to an average of three traditional DMARD agents.

Table 6.1 Rheumatoid Arthritis Subject Demographics

Age in years, mean (SD)	46.4 (15.9)
Female, n (%)	26 (87)
Right Hand Dominant, n (%)	14 (93)
Disease duration in years, mean (SD)	10.6 (11.7)
Disease duration in years, range	1.5 to 46
Rheumatoid Factor positive, %	67
Anti-CCP positive, %	33

DMARD History	
- Average number, mean (SD)	2.8 (1.3)
- Methotrexate, %	93
- Plaquenil, %	100
- Sulfasalazine, %	27
- Gold, %	20
- Leflunomide, %	27
- Biologic therapy, %	40

Legend: SD standard deviation; anti-CCP anti-cyclic citrullinated peptide; DMARD disease modifying anti-rheumatic drug

6.2 Subject Sets for Analysis

For analysis purposes, ten sets of subjects were created based on sex, age and dominant hand (Table 6.2).

Table 6.2 Subject Sets Used in the Quantitative Measures Analysis

Set number	Sex	Hand	Age Group	Number of Subjects in Set
1	Female	Right	19-25	4
2	Female	Right	30-34	2
3	Female	Right	35-39	4
4	Female	Right	40-46	6
5	Female	Left	50-55	2
6	Female	Right	56-59	4
7	Female	Right	60-65	2
8	Female	Right	70-75	2
9	Male	Right	45-50	2
10	Male	Right	65-70	2

6.3 Feasibility

6.3.1 Recruitment and Subject Comfort

Over the course of eleven months, fifteen subjects with RA and fifteen control volunteers underwent x-ray imaging and HR-pQCT scanning of the dominant hand. Scanning time was between twenty to twenty-five minutes for all subjects. Up to one hour was allowed per subject to ensure that they were able to rest between stacks, as long scanning periods could create motion artifact. The scan was well-tolerated, with minor complaints of stiffness occurring after the scan was completed.

6.3.2 Analysis Time

In most subjects with minimal or no motion artifact, all ten joints could be contoured and assessed for image quality within one and a half hours. However, heavily damaged joints and images with significant motion artifact took longer, up to six hours in one instance. Viewing of erosions in each of the ten joints per subject took approximately a half hour. Joint space width measurements and morphometric indices were calculated automatically by the computer software within a matter of minutes.

6.3.3 Image Quality

Table 6.3 summarizes the number of scans of various image qualities observed per joint. As the study progressed, greater attention was placed on the importance of immobility to the subjects. Image quality thus significantly improved. However, 46 of the 299 joints imaged (one 4th MCP was missed inadvertently) (15.4%) were considered unacceptable for joint space width and morphometric indices analysis as they could not be contoured appropriately (grades 4 and 5). In addition, analysis of the joint space width of the IP joint and 1st MCP joint could not be done as the thumb had been positioned too close to the edge of the detection field. Thus when attempting to contour those joints, a software error would occur. Placing the thumb along the palmar surface of the 2nd MCP at the time of image acquisition solved this issue, but not enough scans were available in each set to proceed with analysis. We also identified that scans of the 2nd, 3rd and 4th PIP or MCP joints, where two sequential stacks were imaged, could have discontinuity related to slight motion during the prolonged imaging time (Figure 6.1).

Table 6.3 Image Quality Grade and Number of Scans Available for Each Joint

Image Quality Grade	Total Number by Grade	Distribution - Proximal Interphalangeal (PIP) Joints					Distribution - Metacarpophalangeal (MCP) Joints				
		IP	2nd	3rd	4th	5th	1st	2nd	3rd	4th *	5th
1	163	12	23	24	22	18	4	12	14	16	18
2	62	10	3	3	5	4	13	8	7	5	4
3	28	3	0	0	0	3	7	5	3	3	4
4	17	2	1	2	0	3	1	2	2	3	1
5	29	3	3	1	3	2	5	3	4	2	3

Legend: IP interphalangeal joint of the thumb

* Due to scanning error, the 4th MCP was not imaged for one patient

Figure 6.1 Discontinuities Between Stacks. Slight motion of the hand during scanning results in a discontinuity at the interface of two stacks. This results in overlapping, where the same region of bone is imaged twice (as below) or potentially in a non-imaged gap.

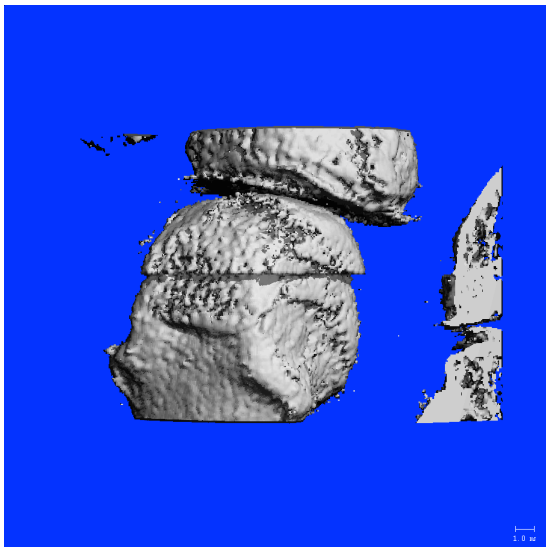

6.4 Quantitative Measurements

6.4.1 Joint Space Width

Using region growing, we were able to ascertain joint space width for all subjects at the 2nd through 5th MCP and PIP joints. This joint space width could also be visualized using planar and three-dimensional images (Figure 6.2). RA subjects had narrowed MCP joints compared to their matched controls at all joints except the 4th PIP joint. A large difference in joint space width between RA subjects and controls was seen at the 2nd MCP joint (mean set difference 250 (standard deviation, SD 282) μm,

paired t-test p=0.0572). Minimal differences in joint space width between RA and control subjects occurred at the other joints, summarized in Table 6.4. The mean joint space width for RA subjects and control subjects are graphed in Figures 6.3 (MCP joints) and 6.4 (PIP joints).

Table 6.4. Joint Space Width Differences Between Rheumatoid Arthritis and Control Subjects

Joint	Mean Difference (SD), μm	Paired t-test p value
2nd MCP	250 (282)	0.0572
3rd MCP	102 (439)	0.5628
4th MCP	39 (415)	0.8116
5th MCP	99 (319)	0.4084
2nd PIP	38 (123)	0.4163
3rd PIP	65 (200)	0.3898
4th PIP	-23 (110)	0.6333
5th PIP	16 (37)	0.3739

Legend: SD Standard Deviation

/C

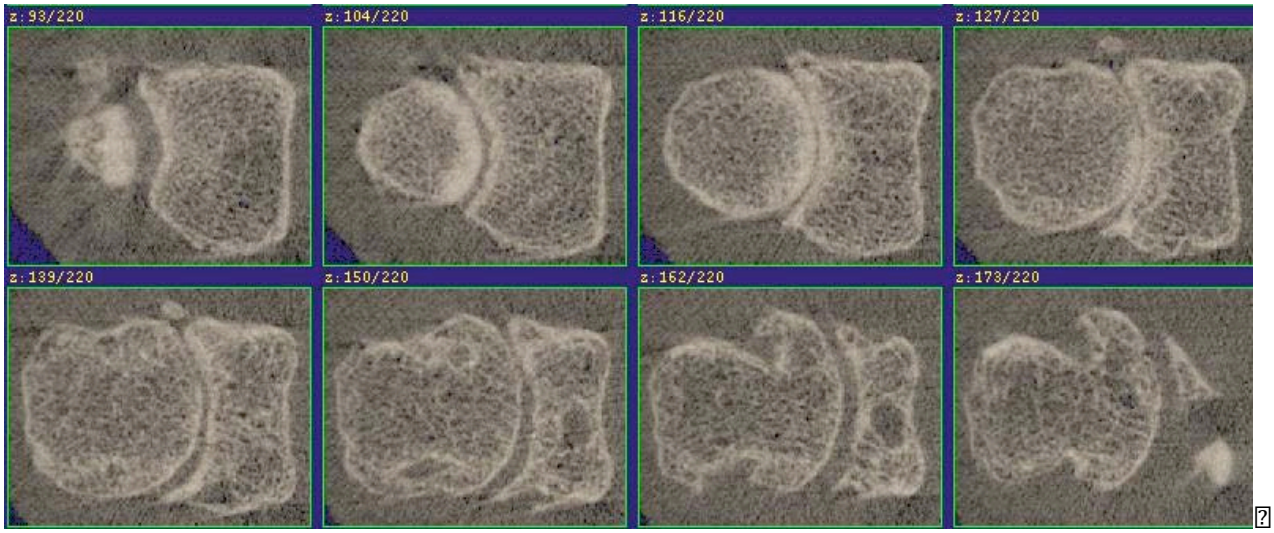
z:93/220
z:104/220
z:116/220
z:127/220
z:139/220
z:150/220
z:162/220
z:173/220

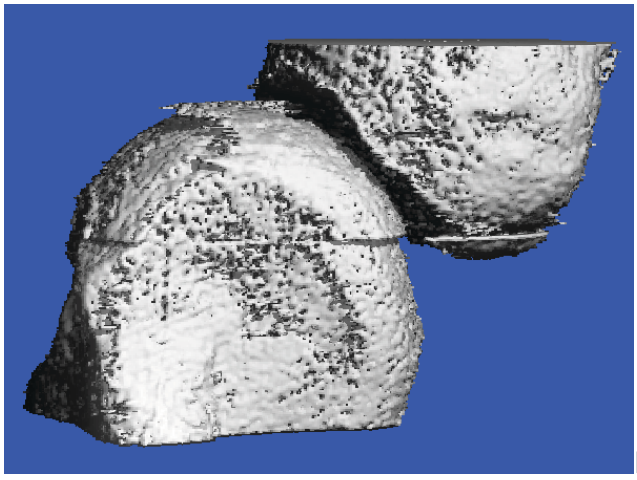

/B

1B rHo IC F: RInde E IC RI: Tnt A Ic : RT

rHo dnC o HRTO: n: r A HRInO RTHRE RI

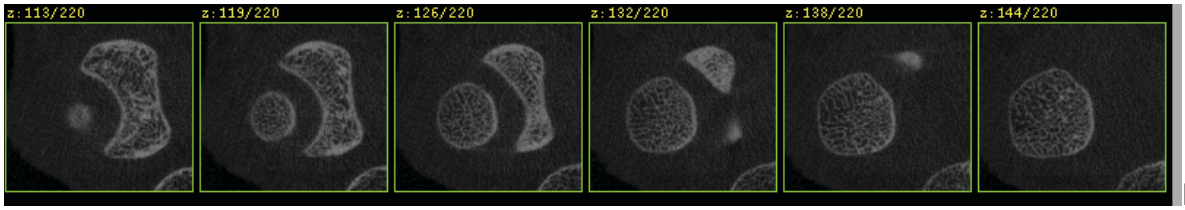

1F rHo IC F: IC RI: Tnt A I

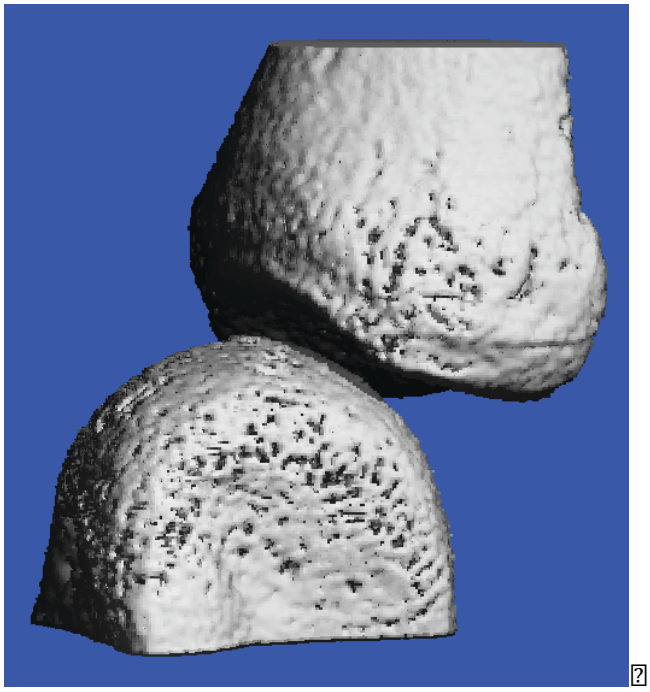

//

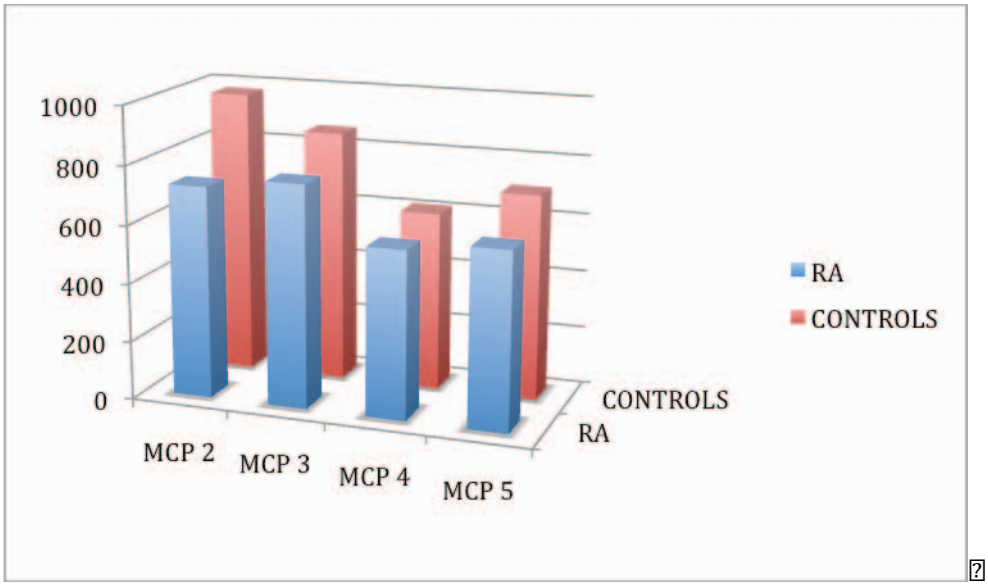
1000
800
600
400
200
0
MCP 2
MCP 3
MCP 4
MCP 5
CONTROLS
RA
RA
CONTROLS

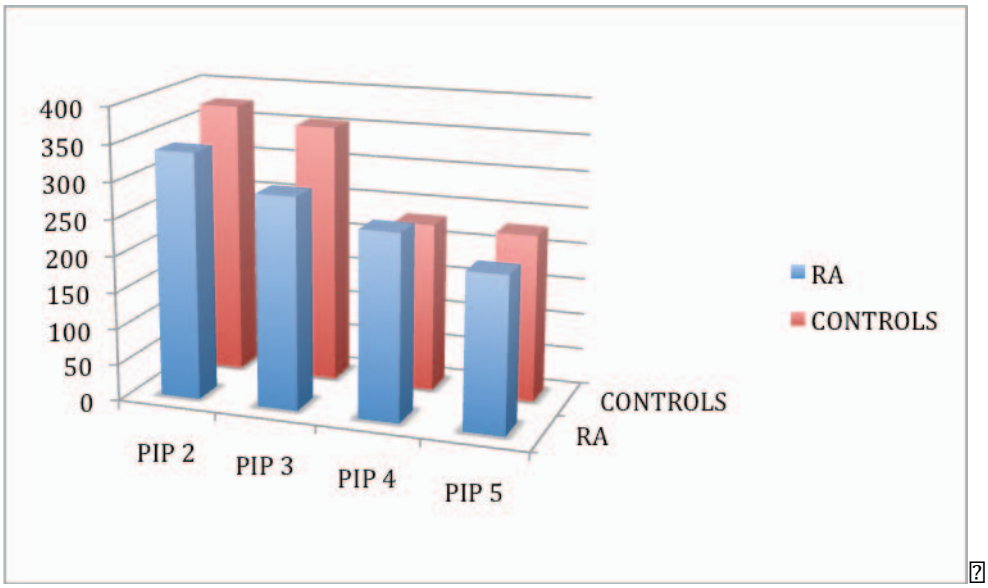
400
350
300
250
200
150
100
50
0
PIP 2
PIP 3
PIP 4
PIP 5
CONTROLS
RA
RA
CONTROLS

6.4.2 Morphometric Indices

The full region of interest (i.e. 60 slices of the metacarpal head and 60 slices of the phalangeal base) was viewed in 18/25 (72%) of the 2nd MCP and 18/24 (75%) of the 3rd MCP images. Morphometric indices of bone volume to total volume ratio, bone density (whole, cortical, trabecular), and specific measurements of cortical thickness, trabecular thickness, trabecular number and trabecular separation were obtained.

RA subjects had a higher mean bone volume/total volume ratio at the 2nd MCP by 6.3% (mean difference 0.037 (SD 0.077), Wilcoxon signed-rank test p=0.6002) and 3rd MCP by 5.3% (mean difference 0.026 (SD 0.058), Wilcoxon signed-rank test p=0.7532). RA subjects had a higher whole bone density by 3.0% at the 2nd MCP joint (mean difference 19.46 (SD 71.54) mg/cm^3, Wilcoxon signed-rank test p=0.6002) and 4.2% at the 3rd MCP (mean difference 20.25 (SD 63.45) mg/cm^3, Wilcoxon signed-rank test p=0.3454).

RA subjects had a lower cortical density at the 2nd MCP by 2.6% (mean difference 14.25 (SD 51.40) mg/cm^3, Wilcoxon signed rank test p=0.4631) but higher at the 3rd MCP by 0.4% (mean difference 6.31 (SD 68.72) mg/cm^3, Wilcoxon signed rank test p=0.7532). Cortical thickness was lower for RA subjects at the 2nd MCP by 2.9% (mean difference 0.006 (SD 0.044) mm, Wilcoxon signed rank test p=0.6002) and at the 3rd MCP by 0.9% (mean difference 0.006 (SD 0.046) mm, Wilcoxon signed rank test p=0.7532).

RA subjects had a higher average trabecular number by 4.8% at the 2nd MCP (mean difference 0.123 (SD 0.189) mm^{-1}, Wilcoxon signed rank test p=0.1159) and by 1.3% at the 3rd MCP (mean difference 0.040 (SD 0.204) mm^{-1}, Wilcoxon signed rank test p=0.6002). Trabecular thickness was also higher in RA subjects, by 2.8% at the 2nd MCP (mean difference 0.011 (SD 0.035) mm, Wilcoxon signed rank test p=0.9165) and 0.8% at the 3rd MCP (mean difference 0.003 (SD 0.018) mm, Wilcoxon signed rank test p=0.7532). Control subjects had wider trabecular separation by 9.4% at the 2nd MCP (mean difference 0.029 (SD 0.047) mm, Wilcoxon signed rank test p=0.1730) and 4.0% at the 3rd MCP (man difference 0.012 (SD 0.045) mm, Wilcoxon signed rank test p=0.4631). Trabecular density was minimally higher in RA subjects by 1.3% at the 2nd MCP (mean difference 10.67 (SD 54.75) mg/cm^3, Wilcoxon signed rank test p=0.6022) and 1.7% at the 3rd MCP (mean difference 9.83 (SD 40.44) mg/cm^3, Wilcoxon signed rank test p=0.6022).

Table 6.5 Morphometric Indices of Rheumatoid Arthritis Subjects Relative to Controls

	Metacarpophalangeal (MCP) Joints	
	2nd	**3rd**
Bone volume/total volume ratio, %		
- RA Subjects, mean (SD)	.477 (.061)	.455 (.025)
- Control Subjects, mean (SD)	.440 (.031)	.429 (.036)
- Mean Difference Between Matched Subjects*, mean (SD)	-.037 (.077)	-.026 (.058)
Whole Bone Density, mg/cm^3		
- RA Subjects, mean (SD)	403.37 (57.57)	379.35 (31.14)
- Control Subjects, mean (SD)	383.91 (31.73)	359.10 (34.39)
- Mean Difference Between Matched Subjects, mean (SD)	-19.46 (71.54)	-20.25 (63.46)
Average cortical thickness, mm		
- RA Subjects, mean (SD)	.328 (.040)	.310 (.031)
- Control Subjects, mean (SD)	.335 (.031)	.304 (.023)

- Mean Difference Between Matched Subjects, mean (SD)	.006 (.044)	-.006 (.046)
Cortical density, mg/cm^3		
- RA Subjects, mean (SD)	647.12 (42.77)	639.28 (45.05)
- Control Subjects, mean (SD)	661.37 (27.81)	632.97 (28.67)
- Mean Difference Between Matched Subjects, mean (SD)	14.25 (51.40)	-6.31 (68.72)
Average trabecular number, mm^{-1}		
- RA Subjects, mean (SD)	2.44 (.15)	2.40 (.15)
- Control Subjects, mean (SD)	2.31 (.15)	2.36 (.11)
- Mean Difference Between Matched Subjects, mean (SD)	-.12 (.19)	-.04 (.20)
Average trabecular thickness, mm		
- RA Subjects, mean (SD)	.284 (.034)	.263 (.014)
- Control Subjects, mean (SD)	.273 (.006)	.261 (.006)
- Mean Difference Between Matched Subjects, mean (SD)	-.011 (.035)	-.003 (.018)
Average trabecular separation, mm		

- RA Subjects, mean (SD)	.338 (.032)	.347 (.026)
- Control Subjects, mean (SD)	.367 (.032)	.359 (.027)
- Mean Difference Between Matched Subjects, mean (SD)	.029 (.047)	.012 (.045)
Trabecular density, mg/cm^3		
- RA Subjects, mean (SD)	519.46 (49.54)	508.95 (22.94)
- Control Subjects, mean (SD)	508.79 (13.82)	499.12 (21.48)
- Mean Difference Between Matched Subjects, mean (SD)	-10.67 (54.75)	-9.83 (40.44)

Legend: SD standard deviation; mg/cm^3 milligrams of hydroxyapatite per cubic centimetre; mm millimeter

* Mean Difference Between Matched Subjects calculated as: (Control Subject Value – RA Subject Value); a negative result indicates that the control subjects had a lower value for that parameter relative to the RA subjects.

6.4.3 Erosion Count and Location

Erosions were found in all RA subjects by HR-pQCT, with an average of 23.6 (SD 17.5) erosions over the ten joints imaged. Nine control subjects were also found to have erosions, with a mean erosion count of 3.6 (SD 5.2) (Table 6.5). Most erosions in

RA subjects occurred at the proximal bone surface of a given joint rather than the distal bone surface (Figure 6.4). In addition, the majority of erosions in RA subjects occurred at the 2nd and 3rd PIP joints, and at the 2nd and 3rd MCP joints. Erosions in control subjects occurred predominantly at distal bone surfaces and at the PIP joints. Figures 6.5 and 6.6 provide examples of erosions seen.

Table 6.6 Presence of Erosions by HR-pQCT

	RA Subject		**Control Subject**	
	PIP Joints	**MCP Joints**	**PIP Joints**	**MCP Joints**
Erosions	15	13	9	7

HEt : 3lS R: nH R t RI : C t E I H2: IC: HHnt A2 In R RI: Thc

u R t : R HRI

1: nH Rn I 1C: dHE T C T Rd c HRIc R

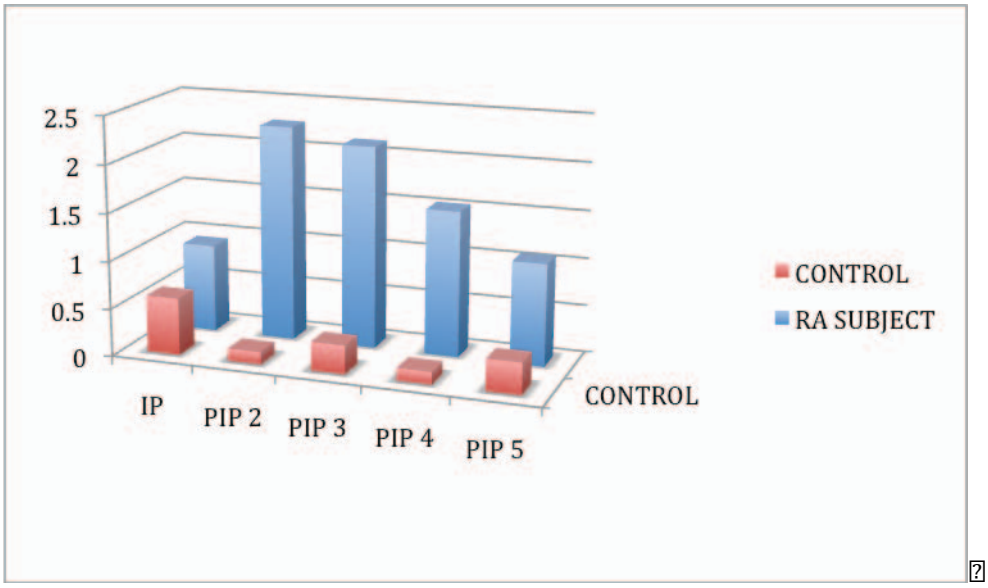

1: nH Rn I 1C H2 T C T Rd nc HRIc R

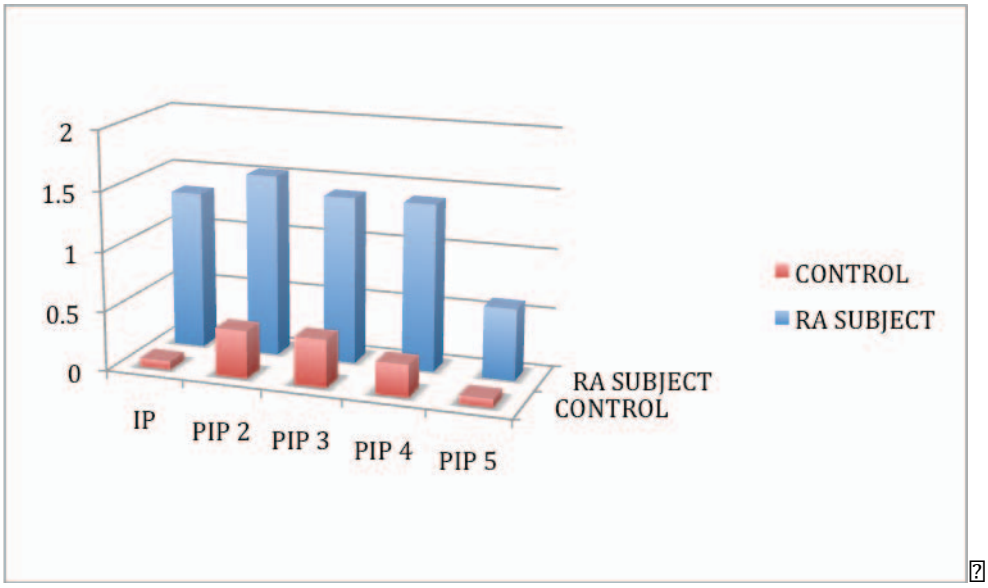

MC

1:

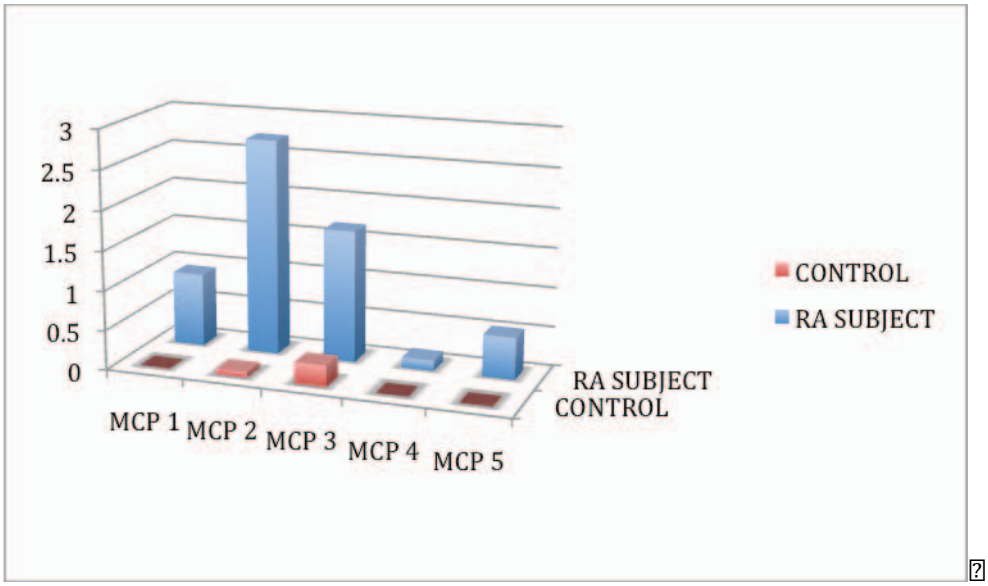
3
2.5
2
1.5
1
0.5
0
MCP 1
MCP 2
MCP 3
MCP 4
MCP 5
CONTROL
RA SUBJECT
RA SUBJECT
CONTROL

1:

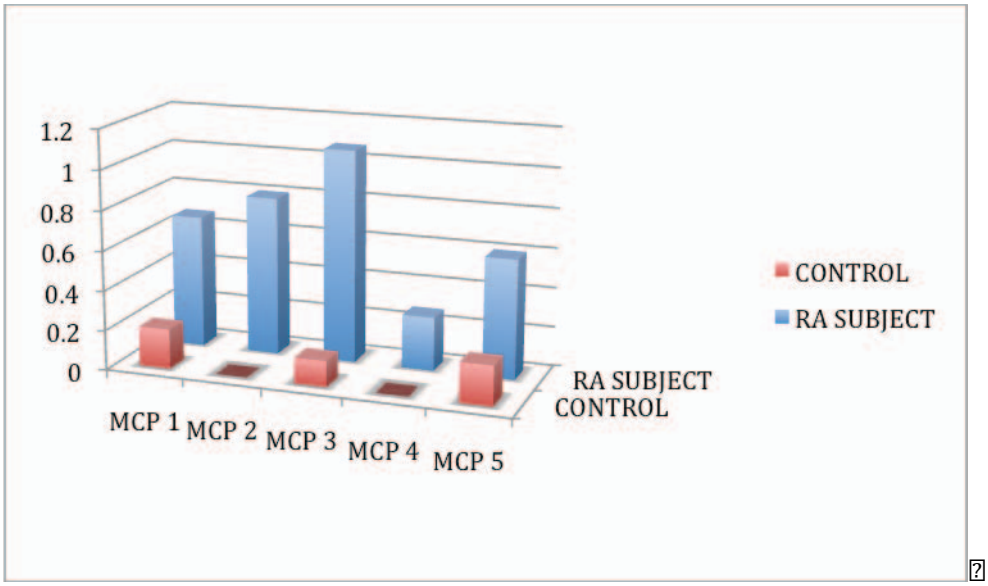
1.2
1
0.8
0.6
0.4
0.2
0
MCP 1
MCP 2
MCP 3
MCP 4
MCP 5
CONTROL
RA SUBJECT
RA SUBJECT
CONTROL

Figure 6.6 Example of Erosions in the 2nd MCP of a Rheumatoid Arthritis Subject, 2D and 3D Views

a) Coronal Plane

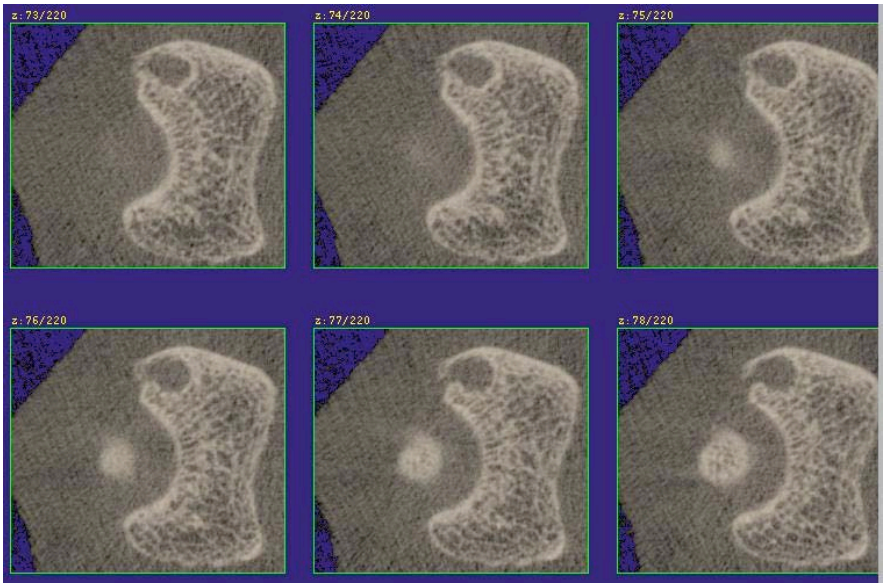

b) Longitudinal Plane

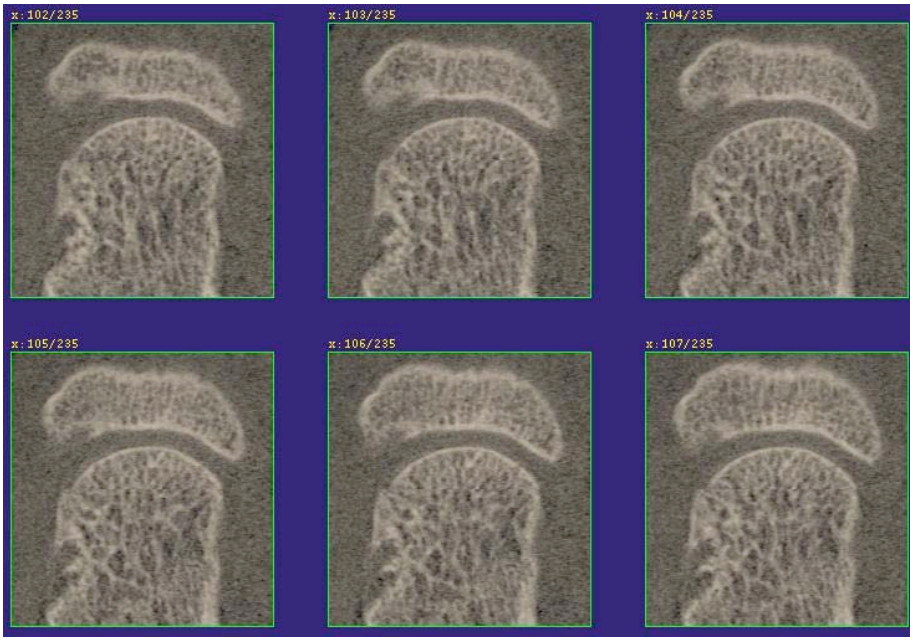

M/

1: Rnr : n T R

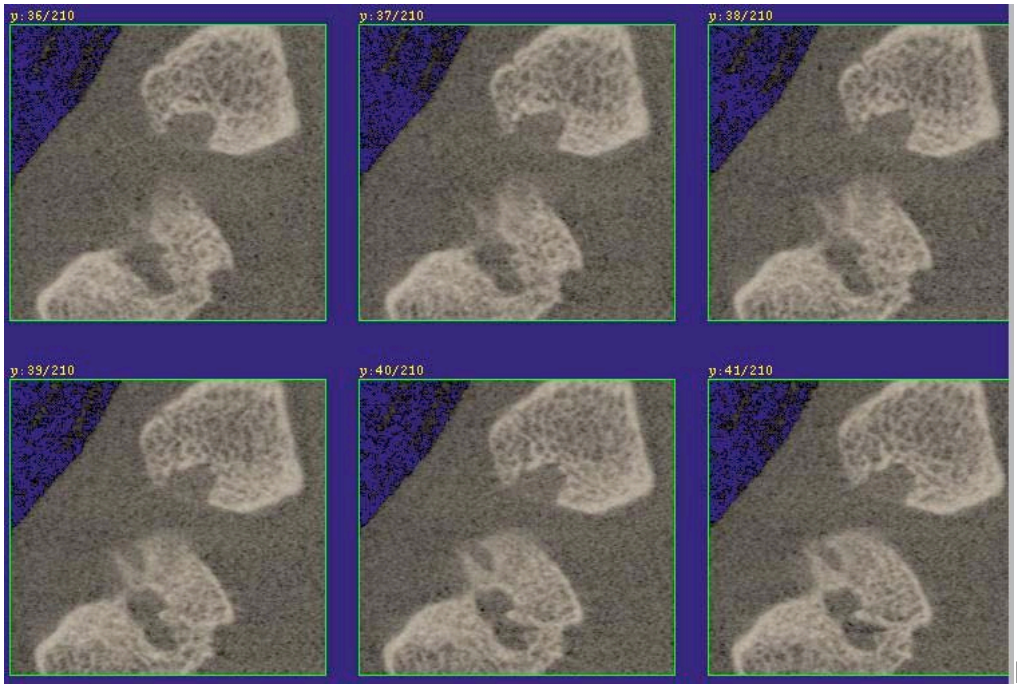

1F rHo lC nE A HRIcnC o HRnt : : nO R HR1 : nH Rn

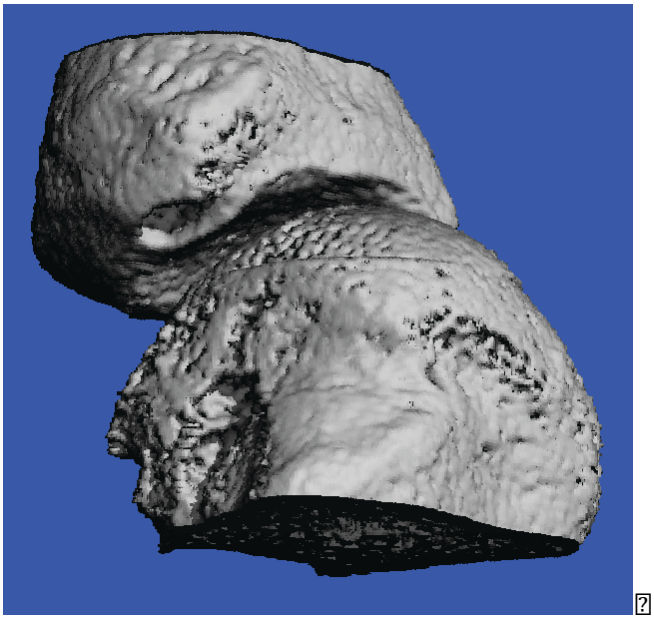

H2t : 3lq : nH R d E OT n

1 r R nI: t IH R IC S IC C t E I H : IC: HHh t A Id

: R T T R

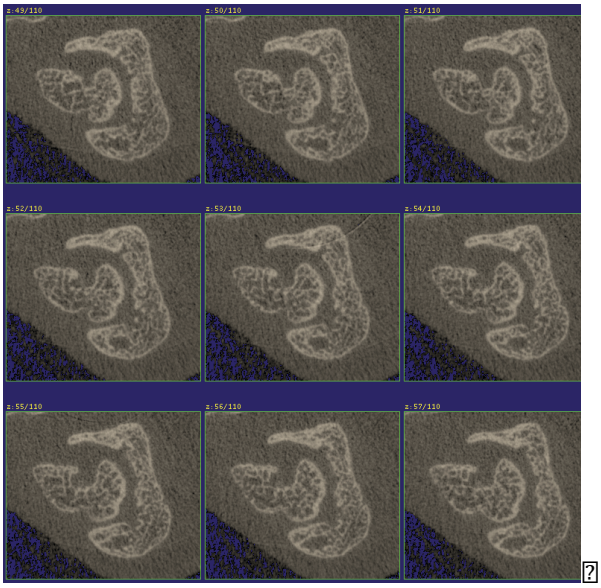

1 r R nI: t IH R IC F: C t E I H : IC: HHh t A Id

: R T T R

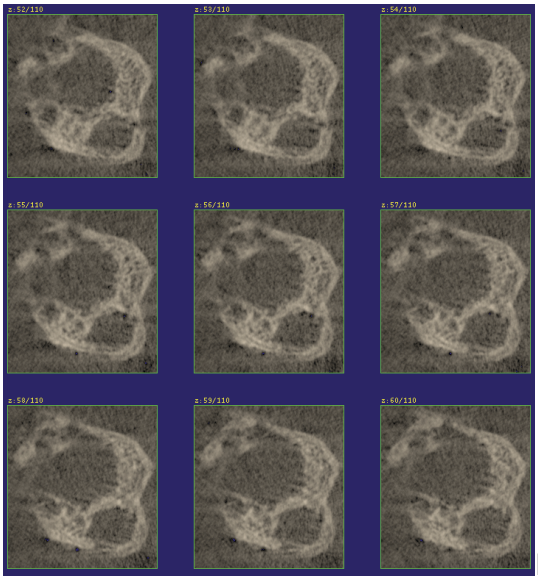

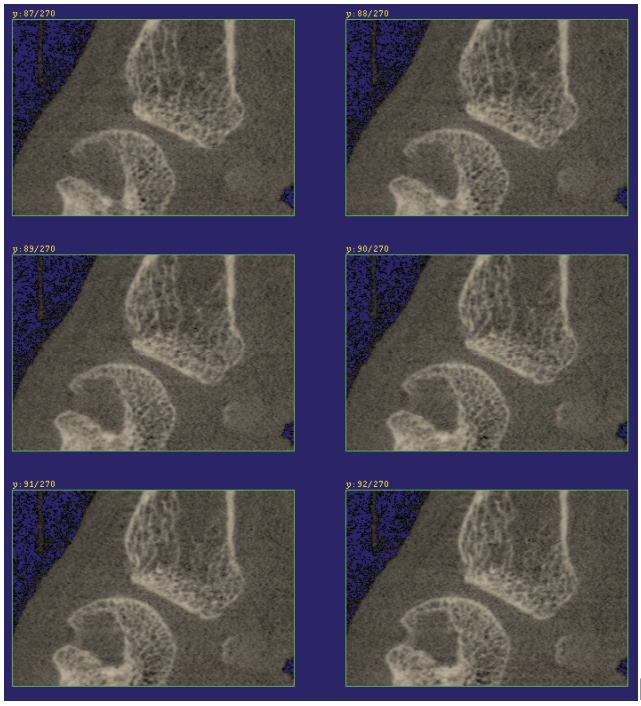
y:87/270
y:88/270
y:89/270
y:90/270
y:91/270
y:92/270

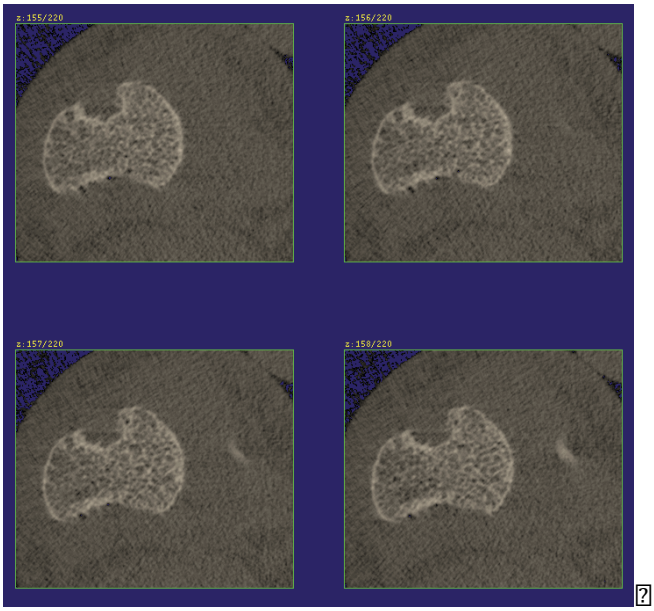
z:155/220
z:156/220
z:157/220
z:158/220

MN

1: nH R R nl OCuI ndB R HRIc : R T R

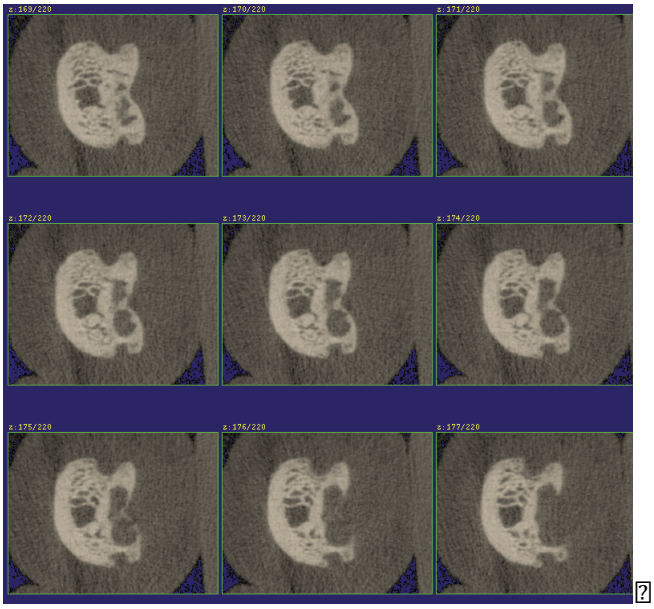

1E HRI ns1c: Rnr : n T R

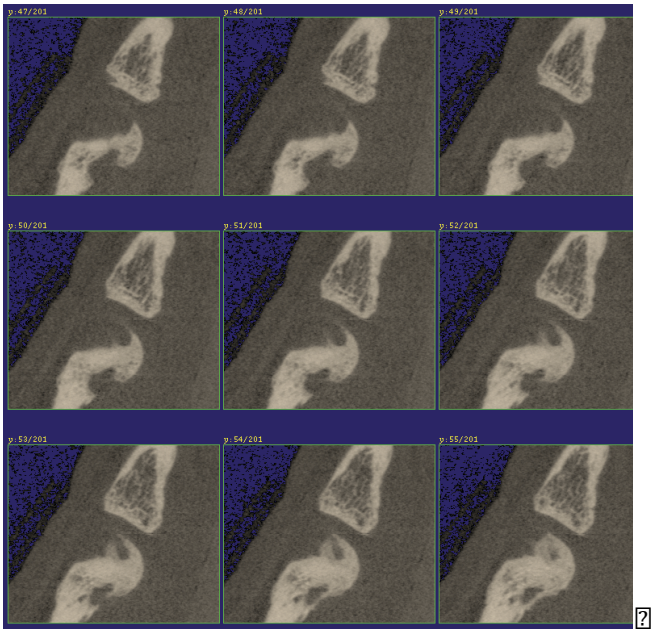

6.4.4 Reproducibility

The root square mean coefficient of variance was calculated using values obtained for joint space width and morphometric indices from two separate contouring evaluations. The root square mean coefficient of variance for joint space width determination was 17.1%. The same joint width was obtained for 22 of the 30 scans (73.3%), with six scans (20.0%) differing by one iteration (total of 164 μm), and two scans (6.7%) differing by two iterations (total of 328 μm). Despite considering factors that could explain the discordant scan results, including subject status (RA or control), image quality, or particular joints, it does not appear that there was any concrete reason for the observed differences (Table 6.6). The root square mean coefficient of variance for morphometric densities was excellent, with all values between 0.13% and 0.83% (Table 6.7).

Table 6.7 Exploratory Analysis for Discordant Results in Joint Space Width

	Number of RA Patients : Number of Controls	**Image Quality**	**Joint**
One Iteration Different (n=6)	2 : 4	Grade 2: n=2 Grade 3: n=4	2nd MCP: n=3 3rd MCP: n=1 4th MCP: n=1 5th PIP: n=1
Two Iterations Different (n=2)	2 : 0	Grade 1: n=2	2nd MCP: n=1 4th MCP: n=1

Table 6.8 Reproducibility of Morphometric Indices

Parameter	**Root Square Mean Coefficient of Variance**
Whole bone density	0.31%
Bone volume/total volume ratio	0.52%
Cortical thickness	0.45%
Cortical density	0.13%
Trabecular number	0.43%
Trabecular thickness	0.83%
Trabecular separation	0.17%
Trabecular density	0.31%

Reproducibility for erosion counts was performed by re-scoring images at least one month after the initial evaluation. The probability of agreement for erosion count was 56.7% (17 of 30 rescored images). The kappa score however was only 0.40, considered to be fair agreement. However, in two-thirds of the scans determined to have non-agreement, there was a variance of only one erosion. Explanatory reasons

1oA hr Ai t sAr(nsr c A ot rh A j ht rn(ht a oshot Ash1 s I h (A Mα%o A t

ht hrsht s oAs n I h (A MN%

Ht : 3 h4 IH R : IH Ii R IC n Rn t IH E nc E IH R n t : n IC

: I d R nt T R Hh : O RI : nH R I : E HR IH Rh

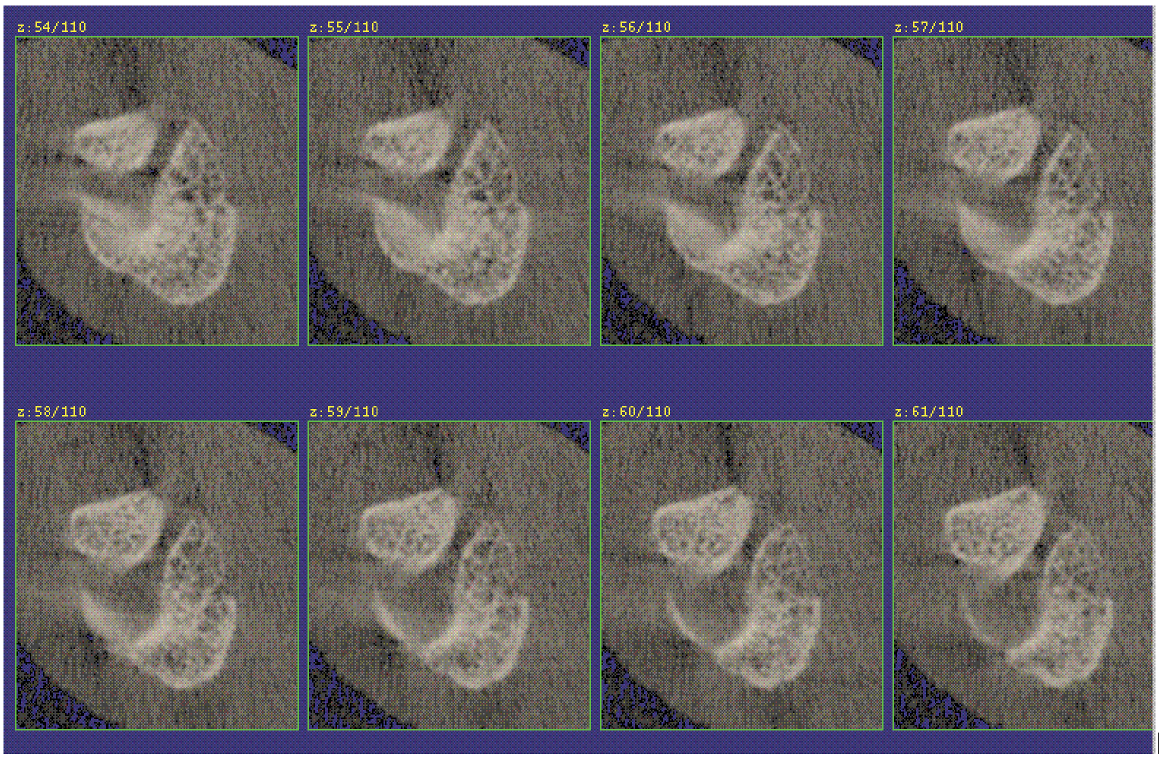

αC

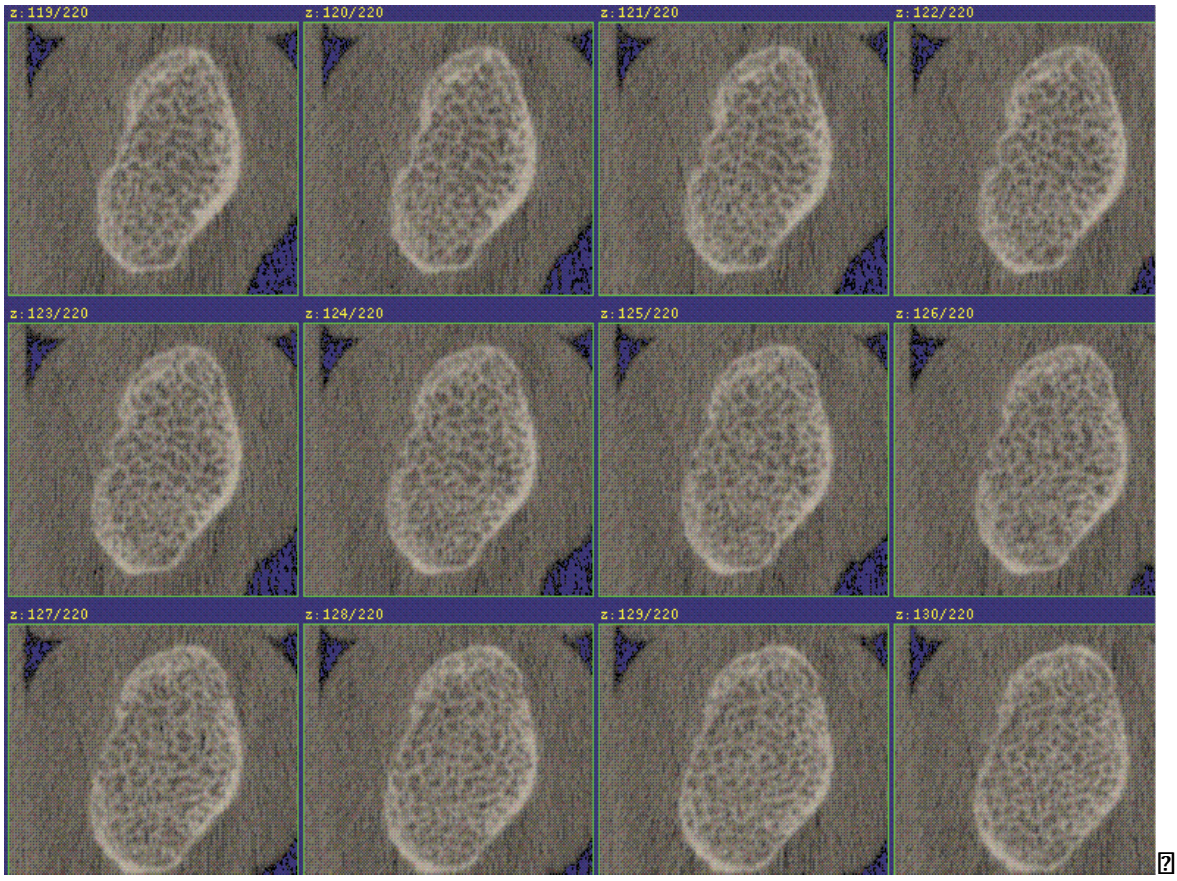
z:119/220
z:120/220
z:121/220
z:122/220
z:123/220
z:124/220
z:125/220
z:126/220
z:127/220
z:128/220
z:129/220
z:130/220

Table 6.9 Inter- and Intra-Rater Reliability For X-Ray Scoring

		Inter-Rater	**Intra-Rater, Reader 1**	**Intra-Rater, Reader 2**
Erosions	Percent agreement	91.0%	92.0%	96.0%
	Kappa	0.7881	0.7642	0.8779

6.5.2 Comparison of Erosion Determination by HR-pQCT and X-Ray

The probability of agreement for both HR-pQCT and x-ray to score erosions at the same joint was 67.5% (n=191/283). Additional erosions, not seen on plain x-ray, were determined by HR-pQCT in 70 joints (24.7%). However, erosions were scored in 22 joints on plain x-ray that were not scored by HR-pQCT (7.8%).

The most obvious reason for discrepancy in erosion determination was related to limited viewing of the 4th MCP joint in HR-pQCT scans. Due to the horizontal alignment of the 2nd, 3rd and 4th MCP joints, only a short portion of the 4th MCP metacarpal head was viewed in most patients. Therefore, 9 of the 22 joints found to have erosions by x-ray but not HR-pQCT were at the 4th MCP joint. The remainder of discrepant joints were evenly distributed (1 at the IP and each of the PIP joints, 1 at each of the 1st and 5th MCP joints, and 3 each at the 2nd and 3rd MCP joints).

The majority of joints found to have erosions by HR-pQCT but not x-ray were PIP joints, with fairly even distribution at each site (8 at the IP, 8 at the 2nd PIP, 8 at the 3rd PIP, 9 at the 4th PIP, 10 at the 5th PIP; 6 at the 1st MCP, 5 at the 2nd MCP, 8 at the 3rd MCP, 2 at the 4th MCP, and 6 at the 5th MCP).

HR-pQCT images with the highest image quality grade detected more erosions. The determination of erosions by HR-pQCT (but not x-ray) occurred in 55 scans scored to be of high quality (grades 1 or 2) but only 15 scans of low quality (grades 3, 4 or 5).

Subject status (i.e. RA or control subject) did not affect erosion determination in terms of discrepant findings between HR-pQCT and x-ray. The determination of erosions by x-ray (but not HR-pQCT) occurred in 12 joints for 8 RA subjects, and in 10 joints for 6 control subjects. The determination of erosions by HR-pQCT (but not x-ray) occurred in 44 joints in 14 RA subjects, and 26 joints in 8 control subjects.

6.6 HR-pQCT as a Diagnostic Test for Rheumatoid Arthritis

Given that joint erosions are diagnostic for RA, and that HR-pQCT is a sensitive technique to identify bony changes at the joints, we wanted to calculate the sensitivity, specificity, and likelihood ratios obtained when using findings of erosions by HR-pQCT to classify subject status (i.e. RA or control subject). Models to evaluate these parameters were created, using findings at a single joint, a combination of joints, and the cumulative number of joints affected. The best model for subject classification

using HR-pQCT was finding an erosion at the 2nd MCP joint, with a sensitivity of 76.9%, specificity of 93.3%, c-statistic 0.851, and a positive likelihood ratio of 11.5 (95%CI 1.7-78.4)) (Table 6.9). The area under the receiver operating curve, or c-statistic, was also maximized when erosions were identified in four, five or six separate joints, or when erosions were found in both the 2nd and 3rd MCPs.

Table 6.10 Model Performance for Erosion Determination by HR-pQCT as a Diagnostic Test for Rheumatoid Arthritis

	Erosion, 2nd MCP	**Erosions, 2nd and 3rd MCPs**	**Erosions, 5 joints**	**Erosions, 6 joints**
Sensitivity	77%	80%	85%	77%
Specificity	93%	73%	80%	87%
C-Statistic	0.851	0.767	0.823	0.818
Positive Likelihood Ratio (95%CI)	11.5 (1.7-78.4)	3.0 (1.3-7.2)	4.2 (1.5-11.9)	5.8 (1.5-21.7)
Negative Likelihood Ratio (95%CI)	0.247 (0.091-0.673)	0.273 (0.095-0.785)	0.192 (0.052-0.705)	0.266 (0.097-0.733)
Positive Predictive Value	91%	75%	79%	83.3%
Negative Predictive Value	82%	79%	86%	81%

αN

3lq IC: E HR HR HR n

t h ts rna ot Rt r c A lo(t c hsR Li ha ht .R r t rf(oAsh s zrsr l h (A M65% ot rrnat r l h (A M66% t mo) rr na R t t m Tl h (A M67% R s R Ao(i mo r Ah r(A1 R t r lt sR hA oAh ht rnal i Aj ssAh(s so1t rsA shot r t sRht t ht ao1sR oAsh rnar(A1 ot C A i A r t s shot Tl h (A M6C%

Ht : 3lf g : I I unl

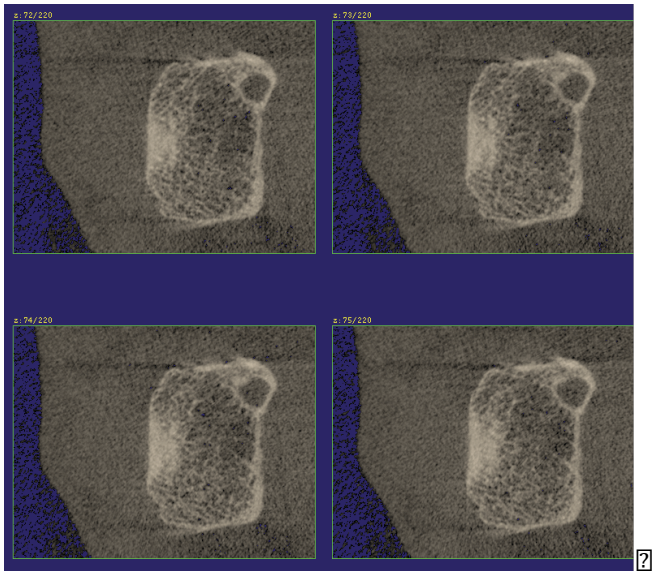

αO

H2t : 3lf f R nT R

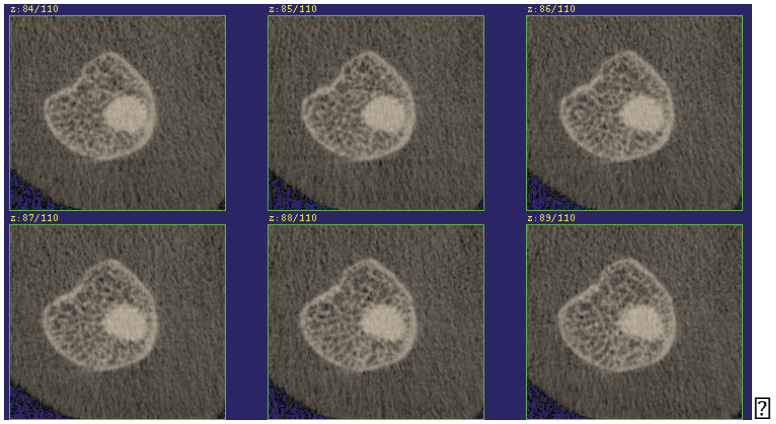

H2t : 3lf B T mn TC RR T

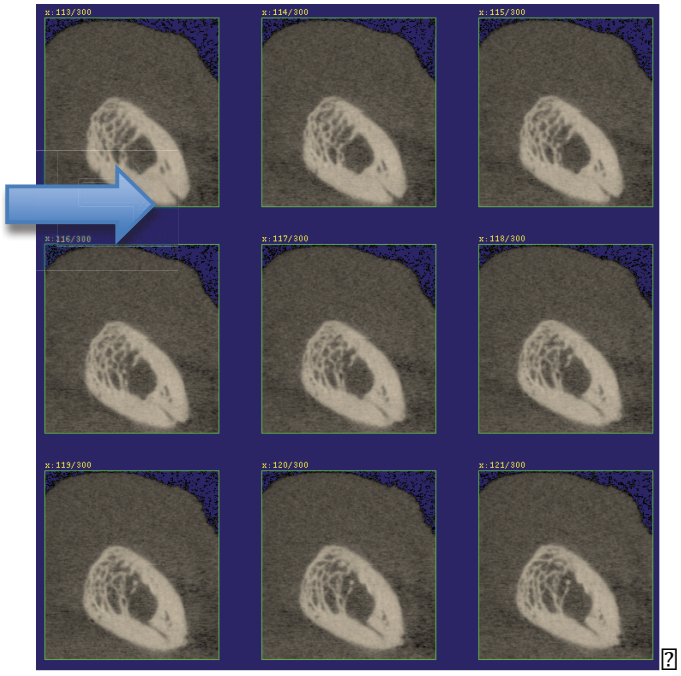

N5

H2t : 3 lf F t : C R n

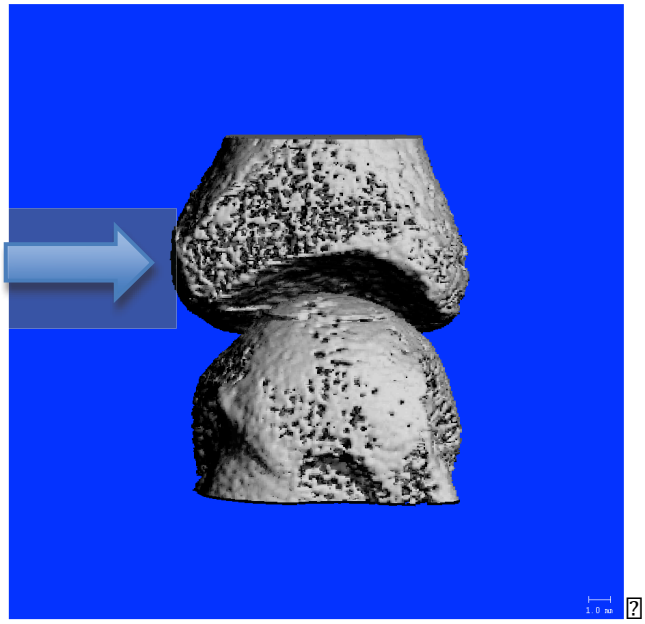

CHAPTER SEVEN: Discussion

Joint damage is a significant cause of functional impairment in RA. Tools that can detect joint damage early, and that are sensitive to change over time, can identify patients requiring aggressive management to optimize outcomes. HR-pQCT is a safe, non-invasive technique, providing high-resolution imaging of the bone. The availability of HR-pQCT technology is increasing in large centers, making this a viable methodology for future clinical use. We have successfully adapted HR-pQCT technology to assess RA joint damage.

7.1 Subject Selection

For this feasibility study, we used subjects with established RA and characteristic findings of chronic structural joint damage by plain radiograph. This was to ensure that disease status was not misclassified, and that we were indeed visualizing well-characterized lesions. All RA subjects in this study were found to have erosive disease, with detectable joint space narrowing by visual inspection and quantitative analysis. Furthermore, subjects with inflamed and damaged joints were able tolerate the scanning procedure. Other studies have also assessed HR-pQCT imaging in patients with established rheumatic diseases. Stach et al characterized erosions in subjects with RA, osteoarthritis and psoriatic arthritis (106). Fouque-

Aubert et al assessed reproducibility in healthy controls, followed by comparative studies among patients with early RA (< 2 years disease duration) and established RA.

Healthy control subjects matched for age-, sex- and dominant-hand were included in this study to account for confounding factors for underlying joint damage. Findings of erosions and joint space narrowing in control subjects likely reflects age-related changes, and highlights that HR-pQCT imaging studies are warranted in both healthy population controls and those with other age-related bony changes such as osteoarthritis to determine what aspects of joint pathology are appropriately attributed to inflammatory arthritis conditions such as RA as opposed to changes expected for degenerative conditions.

7.2 Feasibility of Using HR-pQCT in Rheumatoid Arthritis Damage Assessment

We have demonstrated that HR-pQCT scanning is acceptable to patients in terms of comfort and time commitment. The minimal amount of radiation exposure from HR-pQCT imaging renders this technology safe for repeated assessments over time. All centers to date, including our own, have demonstrated that the highest yield for detecting joint pathology is at the 2nd and 3rd MCP joints, and therefore future protocols should focus on these joints alone. This will decrease the amount of scanning time required (from 25 minutes to 6 minutes) as well as the analysis time necessary to interpret images.

At this time, HR-pQCT remains a research tool available in large urban centers. HR-pQCT scanners have recently been acquired across Canada, including Vancouver, Toronto and Saskatoon. The majority of arthritis and metabolic bone specialists practice in these large centers, and thus there should be reasonable opportunity for patients to participate in future studies. We expect that the number of centers with scanners will continue to grow, and will allow wider access for clinical use once further validity work is performed.

The use of HR-pQCT technology in RA imaging is still in its infancy, and there are no protocols or standards in place for image acquisition and interpretation. To illustrate, each center using HR-pQCT in arthritis research has independently developed hand stabilization platforms to immobilize the joint, and thereby maximize image quality. A commercial product, developed by Pearltec AG, is now available and undergoing evaluation (116). Assessment and determination of the optimal method to address hand stabilization will require a multi-center study. In addition, other centers have altered the manufacturer's default settings for analysis, which could affect image interpretation. We will be hosting a meeting at the University of Calgary in November 2011 to unify the image acquisition and interpretation methodology, and to develop international research collaborations.

7.3 The Benefits of HR-pQCT Imaging in Rheumatoid Arthritis Assessment

HR-pQCT provides high resolution images of bone. The potential to use this technology in longitudinal quantitative assessment of treatment efficacy in RA warrants further investigation, as these quantitative measures may prove superior in accuracy to the current semiquantitative scales in use for assessment of plain radiographs and MRI (117, 118).

7.3.1 Joint Space Width Determination

This study is the first to develop a protocol to quantify the minimum joint space width measurements in 82 μm increments with the hand in anatomical position. The importance of identifying progressive joint narrowing is particularly relevant considering the recent evidence linking joint space narrowing from cartilage loss with declining function over time (119). Additionally, using HR-pQCT to evaluate joint space width is likely superior to the current joint space width determinations attempted with plain radiography and DXR, as the three-dimensional aspect of the joint is taken into account, rather than relying on two-dimensional images.

Differences in joint width measurements were evident between RA and control subjects at the 2nd MCP joint. Longitudinal assessment is needed to determine the natural history of joint space narrowing in disease and health states, as well as the impact of treatment on these measurements. The impact of acute inflammation on joint space width needs to be studied, in particular whether joint width is actually

increased in those with large joint effusions (pseudo-widening). Ideally, this work should be performed in conjunction with an imaging technique recognized for its ability to image soft tissues, such as ultrasound or MRI. The finding of elevated joint space width relative to matched controls may be a useful adjunct to findings of periarticular inflammation and early erosive changes.

Further assessment of the impact of limitations for determining joint space width, such as image quality, fixed flexion deformities and subluxation, are needed. Reproducibility may be affected by differences in positioning with longitudinal studies, and the optimal method to image the joint consistently over time requires further study.

7.3.2 Morphometric Indices

We have demonstrated that periarticular morphometric indices, not currently obtained with standard imaging techniques, can be quantified reproducibly by HR-pQCT technology. These indices are indicative of periarticular osteopenia, which is an important feature of early RA and persistent inflammation. Fouque-Aubert et al found differences in parameters of bone morphometric indices in RA subjects relative to healthy subjects, accounting for age, which is helpful in further understanding the chronic effects of joint damage (109). It is interesting however that this group did not identify differences in morphometric indices based on disease duration, which will require further study.

There are several possible explanations why our study did not detect measurable differences in trabecular and cortical measurements between RA and control subjects. The first is that this study was not powered to detect small differences between groups. For example, 50 patients in each subject arm would be required to detect a 5% difference in trabecular bone density such as that described in the study of Fouque-Aubert et al, with a power of 90% and a one-tailed 5% level of significance. In addition, a larger area of analysis may be required to detect all relevant changes in periarticular bone. Furthermore, we included patients with established disease on stable treatments, who did not have much clinical inflammation. As well, bone density measurements may have been affected by areas of sclerosis or cystic change associated with secondary degenerative changes or be erroneously related to large erosions. Finally, measurements in both subject groups were not corrected for confounding factors for systemic osteopenia or osteoporosis, such as steroid exposure or smoking history.

The other methods for assessing periarticular bone changes, DEXA and DXR (summarized in Pfeil et al), use the mid metacarpal shaft as the region of interest for measurement of bone mineral density, cortical thickness, metacarpal bone width, metacarpal index (ratio of cortical thickness to total bone width) and porosity index (120). These measurements are correlated with functional status, disease activity parameters and erosive changes in RA, and are sensitive to change with treatment. Indeed, future work should compare the results obtained with HR-pQCT and DXR measurements. If these methods are reliably correlated, it would be preferable to use

HR-pQCT as it also provides measures of trabecular bone, with the benefit of three-dimensional viewing for other characteristic bony changes of RA.

7.3.3 Erosion Determination

Erosions are recognized as an important feature in RA diagnosis and prognostication. Comparable to reports from other investigative groups, the number, size and site of erosions can be determined with HR-pQCT technology (106, 107, 109). In this study, the majority of erosions in RA subjects were localized to the metacarpal head of the MCP joints, with an average of 24 erosions over ten joints in those with established disease. In contrast, erosive changes scored in the control subjects were predominantly at the PIP joints.

Similarily, Stach et al determined that the majority of erosive changes in RA subjects occurred at the radial aspect of the metacarpal head, with an erosion depth of >1.9 mm being specific to those with RA (106). Fouque-Aubert et al did not describe the location of erosions but rather provided volume estimates (109). Analysis of erosion depth or volume was not pursued in our study, given that we did not have baseline images for the patients and we would have had to impute where the original periosteal surface may have been. The validity of erosion volume estimates remains controversial.

Finzel et al have explored the characteristics of erosions related to particular types of arthritis (107), and also demonstrated features of normal bony findings, such

as blood vessel channels, which may be confused as erosive changes using other imaging techniques (108). The evidence that the shape and location of erosions are specific to different types of arthritis is strong. We also found that RA erosions were U-shaped, and that findings of damage such as corticated cysts were common in control subjects, likely reflecting osteoarthritis damage in our subjects.

7.3.4 HR-pQCT Performance for Detecting Erosions Compared to Plain Radiograph

Owing to superior resolution and three-dimensional viewing capabilities, more erosions are found by HR-pQCT relative to plain radiography. We found erosions in 24.7% more joints, and it is likely that this is an underestimate given that assessment of the 4th MCP was inadequate. Stach et al found that 58% of the patients with normal radiographs had detectable erosions by HR-pQCT (106). As well, Fouque-Aubert et al found that 7 of 36 early RA patients had erosions of the 2nd MCP by HR-pQCT, and 6 of 36 of the 3rd MCP, despite normal radiographs (109). In patients with established RA, an additional 4 of 14 patients had erosions detected at the 2nd MCP, and 6 of 12 at the 3rd MCP (109).

7.4 HR-pQCT as a Diagnostic Test for Rheumatoid Arthritis

The findings of erosions by HR-pQCT can reliably distinguish RA and control subjects. In particular, we assessed whether the location and number of erosions could distinguish those subjects with RA from healthy controls. Indeed, erosions of the

2nd MCP joint were sensitive (77%) and specific (93%) in RA determination, with a positive predictive value of 91%. The finding of erosions at both the 2nd and 3rd MCP joints performed equally to finding erosions in any four joints (sensitivity 80%, specificity 73%, positive predictive value 79%). Finding erosions in five or six joints also provided good test characteristics, but beyond that the sensitivity was lowered.

The only other group to look at the discrimination power of HR-pQCT was Stach et al. They created models combining semiquantitative scores for erosions, surface changes and osteophytes (106). The best capability of determining healthy controls from RA subjects was a composite score combining the square of the erosion score with the surface change score and osteophyte score. However, a composite score of only the square of the erosion score and surface change score was suggested for use given the difficulties of scoring osteophytes.

7.5 Study Strengths

The results of this study add important data to a growing body of literature validating the use of HR-pQCT for imaging RA joint damage. We enrolled subjects with established disease to eliminate misclassification of subject status, and to ensure that findings were specific to RA damage. With respect to feasibility, we have considered patient comfort and time commitment, analysis time and reproducibility, with the view of the potential for widespread uptake of this technique in both settings of research and clinical practice. We provide the first methodology for assessing joint

space width, an important consideration for functional outcomes. We have exploited the quantitative capabilities of HR-pQCT in measuring periarticular morphometric indices, considering confounding factors of age, sex, and dominant hand use, which could provide important prognostic information in those with active inflammatory disease. We provide further data on the sensitivity of HR-pQCT to determine erosions relative to plain radiography, and that erosions can differentiate subjects with RA from controls.

7.6 Study Limitations

The sample size challenged our ability to detect demonstrable differences between RA and control subjects, and normative data will be necessary for further comparative studies. We did not account for occupations or hobbies that may affect joint microstructure, nor did we correct for differences in bone surface area between subjects. We could not reliably account for the cumulative disease burden in the RA subjects, as this was a cross-sectional assessment without prospectively collected clinical data. Our reproducibility for joint space width measurements could be improved, and we are committed to continuing reproducibility work and optimizing techniques for immobilization and standardization.

7.7 Importance and Potential Applications for HR-pQCT

There is clearly great potential for HR-pQCT imaging in patients with inflammatory arthritis. This highly sensitive imaging technique can detect the earliest stages of erosions, allowing improved prognostication and therefore informing management of those with early inflammatory arthritis. As well, in patients presenting with arthralgias but without detectable synovitis, the lack of erosive changes may reassure the patient and physician that observation is appropriate rather than initiating aggressive medical therapy. Current and future research in our lab will focus specifically on HR-pQCT imaging features in patients with early RA and undifferentiated arthritis, with the goal of combining information on erosions and periarticular morphometric indices to serve as biomarkers.

HR-pQCT imaging appears to be useful for further evaluation of erosion characteristics particular to different types of arthritis. It is anticipated that longitudinal evaluations in individuals will provide information on disease progression and treatment efficacy, as well as the natural history of erosion healing and joint space narrowing. Image acquisition techniques to ensure consistency in the area viewed over time will be developed.

Radiographic outcomes are of primary importance in RA clinical trials. The ability to detect small differences in erosion and joint space narrowing will increase the power of clinical trials of therapeutic agents, and reduce the number of patients needed to determine treatment efficacy.

7.8 Conclusion

This feasibility study demonstrated that HR-pQCT is easily performed and is suitable for patient evaluation. We have exploited the quantitative features of this technology, calculating joint space widths and morphometric indices. We have also determined erosion counts and locations, and demonstrated superiority in viewing erosions relative to plain radiographs. Finally, this technology allowed us to reproducibly distinguish RA subjects from healthy controls based on erosion determination. HR-pQCT technology holds great promise in the investigation of bony damage in inflammatory arthritis and may prove to be superior to currently available imaging techniques, not only for detecting erosive changes but also for safely following quantitative measures of joint space width and morphologic indices longitudinally.

REFERENCES

1. Klarenbeek NB, Kerstens PJ, Huizinga TW, Dijkmans BA, Allaart CF. Recent advances in the management of rheumatoid arthritis. BMJ. 2010 Dec 21;341:c6942.

2. Myasoedova E, Crowson CS, Kremers HM, Therneau TM, Gabriel SE. Is the incidence of rheumatoid arthritis rising?: Results from Olmsted County, Minnesota, 1955-2007. Arthritis Rheum. 2010 Jun;62(6):1576-82.

3. Alamanos Y, Voulgari PV, Drosos AA. Incidence and prevalence of rheumatoid arthritis, based on the 1987 American College of Rheumatology criteria: A systematic review. Semin Arthritis Rheum. 2006 Dec;36(3):182-8.

4. Cooles FA, Isaacs JD. Pathophysiology of rheumatoid arthritis. Curr Opin Rheumatol. 2011 May;23(3):233-40.

5. Shiozawa S, Tsumiyama K, Yoshida K, Hashiramoto A. Pathogenesis of joint destruction in rheumatoid arthritis. Arch Immunol Ther Exp. 2011;59:89-95.

6. Goldring MB, Marcu KB. Cartilage homeostasis in health and rheumatic diseases. Arthritis Res Ther. 2009;11(3):224.

7. Schett G. Osteoimmunology in rheumatic diseases. Arthritis Res Ther. 2009;11(1):210.

8. Karmakar S, Kay J, Gravallese EM. Bone damage in rheumatoid arthritis: Mechanistic insights and approaches to prevention. Rheum Dis Clin North Am. 2010 May;36(2):385-404.

9. van der Heijde DM. Radiographic imaging: The 'gold standard' for assessment of disease progression in rheumatoid arthritis. Rheumatology (Oxford). 2000 Jun;39 Suppl 1:9-16.

10. van der Heijde D. Radiographic progression in rheumatoid arthritis: Does it reflect outcome? Does it reflect treatment? Ann Rheum Dis. 2001 Nov;60 Suppl 3:iii47-50.

11. Clarke AE, St-Pierre Y, Joseph L, Penrod J, Sibley JT, Haga M, et al. Radiographic damage in rheumatoid arthritis correlates with functional disability but not direct medical costs. J Rheumatol. 2001 Nov;28(11):2416-24.

12. Kirwan JR. Links between radiological change, disability, and pathology in rheumatoid arthritis. J Rheumatol. 2001 Apr;28(4):881-6.

13. Welsing PM, Landewe RB, van Riel PL, Boers M, van Gestel AM, van der Linden S, et al. The relationship between disease activity and radiologic progression in patients with rheumatoid arthritis: A longitudinal analysis. Arthritis Rheum. 2004 Jul;50(7):2082-93.

14. Avina-Zubieta JA, Choi HK, Sadatsafavi M, Etminan M, Esdaile JM, Lacaille D. Risk of cardiovascular mortality in patients with rheumatoid arthritis: A meta-analysis of observational studies. Arthritis Rheum. 2008 Dec 15;59(12):1690-7.

15. Myasoedova E, Davis JM,3rd, Crowson CS, Gabriel SE. Epidemiology of rheumatoid arthritis: Rheumatoid arthritis and mortality. Curr Rheumatol Rep. 2010 Oct;12(5):379-85.

16. Michaud K, Messer J, Choi HK, Wolfe F. Direct medical costs and their predictors in patients with rheumatoid arthritis: A three-year study of 7,527 patients. Arthritis Rheum. 2003 Oct;48(10):2750-62.

17. Neovius M, Simard JF, Askling J, for the ARTIS Study Group. How large are the productivity losses in contemporary patients with RA, and how soon in relation to diagnosis do they develop? Ann Rheum Dis. 2011 Jun;70(6):1010-5.

18. Lindqvist E, Jonsson K, Saxne T, Eberhardt K. Course of radiographic damage over 10 years in a cohort with early rheumatoid arthritis. Ann Rheum Dis. 2003 Jul;62(7):611-6.

19. Fuchs HA, Kaye JJ, Callahan LF, Nance EP, Pincus T. Evidence of significant radiographic damage in rheumatoid arthritis within the first 2 years of disease. J Rheumatol. 1989 May;16(5):585-91.

20. Quinn MA, Green MJ, Conaghan P, Emery P. How do you diagnose rheumatoid arthritis early? Best Pract Res Clin Rheumatol. 2001 Mar;15(1):49-66.

21. van der Linden MP, le Cessie S, Raza K, van der Woude D, Knevel R, Huizinga TW, et al. Long-term impact of delay in assessment of patients with early arthritis. Arthritis Rheum. 2010 Dec;62(12):3537-46.

22. Hazes JM, Luime JJ. The epidemiology of early inflammatory arthritis. Nat Rev Rheumatol. 2011 Jun;7(7):381-90.

23. Suter LG, Fraenkel L, Braithwaite S. Cost-effectiveness of adding magnetic resonance imaging to rheumatoid arthritis management. Arch Intern Med. 2011;171(7):657-667.

24. Wolfe F, Ross K, Hawley DJ, Roberts FK, Cathey MA. The prognosis of rheumatoid arthritis and undifferentiated polyarthritis syndrome in the clinic: A study of 1141 patients. J Rheumatol. 1993 Dec;20(12):2005-9.

25. Knevel R, Schoels M, Huizinga TW, Aletaha D, Burmester GR, Combe B, et al. Current evidence for a strategic approach to the management of rheumatoid arthritis with disease-modifying antirheumatic drugs: A systematic literature review informing the EULAR recommendations for the management of rheumatoid arthritis. Ann Rheum Dis. 2010 Jun;69(6):987-94.

26. Bell MJ, Tavares R, Guillemin F, Bykerk VP, Tugwell P, Wells GA. Development of a self-administered early inflammatory arthritis detection tool. BMC Musculoskelet Disord. 2010 Mar 17;11:50.

27. Quinn MA, Emery P. Are early arthritis clinics necessary? Best Pract Res Clin Rheumatol. 2005 Feb;19(1):1-17.

28. van der Helm-van Mil AH, le Cessie S, van Dongen H, Breedveld FC, Toes RE, Huizinga TW. A prediction rule for disease outcome in patients with recent-onset undifferentiated arthritis: How to guide individual treatment decisions. Arthritis Rheum. 2007 Feb;56(2):433-40.

29. Pruijn GJ, Wiik A, van Venrooij WJ. The use of citrullinated peptides and proteins for the diagnosis of rheumatoid arthritis. Arthritis Res Ther. 2010;12(1):203.

30. McGonagle D, Conaghan PG, Wakefield R, Emery P. Imaging the joints in early rheumatoid arthritis. Best Pract Res Clin Rheumatol. 2001 Mar;15(1):91-104.

31. Boutry N, Larde A, Lapegue F, Solau-Gervais E, Flipo RM, Cotten A. Magnetic resonance imaging appearance of the hands and feet in patients with early rheumatoid arthritis. J Rheumatol. 2003 Apr;30(4):671-9.

32. Lindegaard HM, Vallo J, Horslev-Petersen K, Junker P, Ostergaard M. Low-cost, low-field dedicated extremity magnetic resonance imaging in early rheumatoid arthritis: A 1-year follow-up study. Ann Rheum Dis. 2006 Sep;65(9):1208-12.

33. Klarlund M, Ostergaard M, Jensen KE, Madsen JL, Skjodt H, Lorenzen I. Magnetic resonance imaging, radiography, and scintigraphy of the finger joints: One year follow up of patients with early arthritis. The TIRA group. Ann Rheum Dis. 2000 Jul;59(7):521-8.

34. Sugimoto H, Takeda A, Hyodoh K. Early-stage rheumatoid arthritis: Prospective study of the effectiveness of MR imaging for diagnosis. Radiology. 2000 Aug;216(2):569-75.

35. Calisir C, Murat Aynaci AI, Korkmaz C. The accuracy of magnetic resonance imaging of the hands and feet in the diagnosis of early rheumatoid arthritis. Joint Bone Spine. 2007 Jul;74(4):362-7.

36. Naredo E, Collado P, Cruz A, Palop MJ, Cabero F, Richi P, et al. Longitudinal power doppler ultrasonographic assessment of joint inflammatory activity in early rheumatoid arthritis: Predictive value in disease activity and radiologic progression. Arthritis Rheum. 2007 Feb 15;57(1):116-24.

37. Bottcher J, Pfeil A, Rosholm A, Petrovitch A, Seidl BE, Malich A, et al. Digital X-ray radiogrammetry combined with semiautomated analysis of joint space widths as a new diagnostic approach in rheumatoid arthritis: A cross-sectional and longitudinal study. Arthritis Rheum. 2005 Dec;52(12):3850-9.

38. Bottcher J, Pfeil A, Rosholm A, Schafer ML, Malich A, Petrovitch A, et al. Computerized digital imaging techniques provided by digital X-ray radiogrammetry as new diagnostic tool in rheumatoid arthritis. J Digit Imaging. 2006 Sep;19(3):279-88.

39. Bottcher J, Pfeil A, Rosholm A, Soros P, Petrovitch A, Schaefer ML, et al. Computerized quantification of joint space narrowing and periarticular demineralization in patients with rheumatoid arthritis based on digital x-ray radiogrammetry. Invest Radiol. 2006 Jan;41(1):36-44.

40. Landewe R. Predictive markers in rapidly progressing rheumatoid arthritis. J Rheumatol Suppl. 2007 Nov;80:8-15.

41. Boers M, Kostense PJ, Verhoeven AC, van der Linden S, COBRA Trial Group. Combinatietherapie Bij Reumatoide Artritis. Inflammation and damage in an

individual joint predict further damage in that joint in patients with early rheumatoid arthritis. Arthritis Rheum. 2001 Oct;44(10):2242-6.

42. Belghomari H, Saraux A, Allain J, Guedes C, Youinou P, Le Goff P. Risk factors for radiographic articular destruction of hands and wrists in rheumatoid arthritis. J Rheumatol. 1999 Dec;26(12):2534-8.

43. Dixey J, Solymossy C, Young A, Early RA Study. Is it possible to predict radiological damage in early rheumatoid arthritis (RA)? A report on the occurrence, progression, and prognostic factors of radiological erosions over the first 3 years in 866 patients from the early RA study (ERAS). J Rheumatol Suppl. 2004 Mar;69:48-54.

44. Berglin E, Johansson T, Sundin U, Jidell E, Wadell G, Hallmans G, et al. Radiological outcome in rheumatoid arthritis is predicted by presence of antibodies against cyclic citrullinated peptide before and at disease onset, and by IgA-RF at disease onset. Ann Rheum Dis. 2006 Apr;65(4):453-8.

45. Linn-Rasker SP, van der Helm-van Mil AH, Breedveld FC, Huizinga TW. Arthritis of the large joints - in particular, the knee - at first presentation is predictive for a high level of radiological destruction of the small joints in rheumatoid arthritis. Ann Rheum Dis. 2007 May;66(5):646-50.

46. Guillemin F, Gerard N, van Leeuwen M, Smedstad LM, Kvien TK, van den Heuvel W, et al. Prognostic factors for joint destruction in rheumatoid arthritis: A prospective longitudinal study of 318 patients. J Rheumatol. 2003 Dec;30(12):2585-9.

47. Mottonen TT. Prediction of erosiveness and rate of development of new erosions in early rheumatoid arthritis. Ann Rheum Dis. 1988 Aug;47(8):648-53.

48. Machold KP, Stamm TA, Nell VP, Pflugbeil S, Aletaha D, Steiner G, et al. Very recent onset rheumatoid arthritis: Clinical and serological patient characteristics associated with radiographic progression over the first years of disease. Rheumatology (Oxford). 2007 Feb;46(2):342-9.

49. Kaufmann J, Kielstein V, Kilian S, Stein G, Hein G. Relation between body mass index and radiological progression in patients with rheumatoid arthritis. J Rheumatol. 2003 Nov;30(11):2350-5.

50. Westhoff G, Rau R, Zink A. Radiographic joint damage in early rheumatoid arthritis is highly dependent on body mass index. Arthritis Rheum. 2007 Nov;56(11):3575-82.

51. van der Helm-van Mil AH, van der Kooij SM, Allaart CF, Toes RE, Huizinga TW. A high body mass index has a protective effect on the amount of joint destruction in small joints in early rheumatoid arthritis. Ann Rheum Dis. 2008 Jun;67(6):769-74.

52. Forslind K, Keller C, Svensson B, Hafstrom I, BARFOT Study Group. Reduced bone mineral density in early rheumatoid arthritis is associated with radiological joint damage at baseline and after 2 years in women. J Rheumatol. 2003 Dec;30(12):2590-6.

53. Garnero P, Landewe R, Boers M, Verhoeven A, Van Der Linden S, Christgau S, et al. Association of baseline levels of markers of bone and cartilage degradation with long-

term progression of joint damage in patients with early rheumatoid arthritis: The COBRA study. Arthritis Rheum. 2002 Nov;46(11):2847-56.

54. Jansen LM, van der Horst-Bruinsma I, Lems WF, van Schaardenburg D, van de Stadt R, de Koning M, et al. Serological bone markers and joint damage in early polyarthritis. J Rheumatol. 2004 Aug;31(8):1491-6.

55. Bukhari M, Lunt M, Harrison BJ, Scott DG, Symmons DP, Silman AJ. Erosions in inflammatory polyarthritis are symmetrical regardless of rheumatoid factor status: Results from a primary care-based inception cohort of patients. Rheumatology (Oxford). 2002 Mar;41(3):246-52.

56. Kapetanovic MC, Lindqvist E, Algulin J, Jonsson K, Saxne T, Eberhardt K, et al. Early changes in bone mineral density measured by digital X-ray radiogrammetry predict up to 20 years radiological outcome in rheumatoid arthritis. Arthritis Res Ther. 2011;13(1):R31.

57. Boini S, Guillemin F. Radiographic scoring methods as outcome measures in rheumatoid arthritis: Properties and advantages. Ann Rheum Dis. 2001 Sep;60(9):817-27.

58. Sharp JT, van der Heijde D, Angwin J, Duryea J, Moens HJ, Jacobs JW, et al. Measurement of joint space width and erosion size. J Rheumatol. 2005 Dec;32(12):2456-61.

59. Taouli B, Guermazi A, Sack KE, Genant HK. Imaging of the hand and wrist in RA. Ann Rheum Dis. 2002 Oct;61(10):867-9.

60. Tan AL, Wakefield RJ, Conaghan PG, Emery P, McGonagle D. Imaging of the musculoskeletal system: Magnetic resonance imaging, ultrasonography and computed tomography. Best Pract Res Clin Rheumatol. 2003 Jun;17(3):513-28.

61. Savnik A, Malmskov H, Thomsen HS, Graff LB, Nielsen H, Danneskiold-Samsoe B, et al. Magnetic resonance imaging of the wrist and finger joints in patients with inflammatory joint diseases. J Rheumatol. 2001 Oct;28(10):2193-200.

62. Perry D, Stewart N, Benton N, Robinson E, Yeoman S, Crabbe J, et al. Detection of erosions in the rheumatoid hand; a comparative study of multidetector computerized tomography versus magnetic resonance scanning. J Rheumatol. 2005 Feb;32(2):256-67.

63. Ravindran V, Rachapalli S. An overview of commonly used radiographic scoring methods in rheumatoid arthritis clinical trials. Clin Rheumatol. 2010 Aug 21.

64. Ejbjerg B, Narvestad E, Rostrup E, Szkudlarek M, Jacobsen S, Thomsen HS, et al. Magnetic resonance imaging of wrist and finger joints in healthy subjects occasionally shows changes resembling erosions and synovitis as seen in rheumatoid arthritis. Arthritis Rheum. 2004 Apr;50(4):1097-106.

65. Szkudlarek M, Klarlund M, Narvestad E, Court-Payen M, Strandberg C, Jensen KE, et al. Ultrasonography of the metacarpophalangeal and proximal interphalangeal joints in rheumatoid arthritis: A comparison with magnetic resonance imaging, conventional radiography and clinical examination. Arthritis Res Ther. 2006;8(2):R52.

66. Moller Dohn U, Ejbjerg B, Hasselquist M, Narvestad E, Court-Payen M, Szkudlarek M, et al. Rheumatoid arthritis bone erosion volumes on CT and MRI: Reliability and correlations with erosion scores on CT, MRI and radiography. . 2007;66:1388--1392.

67. Moller Dohn U, Boonen A, Hetland ML, Hansen MS, Knudsen LS, Hansen A, et al. Erosive progression is minimal, but erosion healing rare, in patients with rheumatoid arthritis treated with adalimumab. A 1 year investigator-initiated follow-up study using high-resolution computed tomography as the primary outcome measure. Ann Rheum Dis. 2009 Oct;68(10):1585-90.

68. Larsen A. How to apply Larsen score in evaluating radiographs of rheumatoid arthritis in long-term studies. J Rheumatol. 1995 Oct;22(10):1974-5.

69. Sharp JT, Young DY, Bluhm GB, Brook A, Brower AC, Corbett M, et al. How many joints in the hands and wrists should be included in a score of radiologic abnormalities used to assess rheumatoid arthritis? Arthritis Rheum. 1985 Dec;28(12):1326-35.

70. van der Heijde D. How to read radiographs according to the Sharp/van der heijde method. J Rheumatol. 1999 Mar;26(3):743-5.

71. Higgs JB, Smith D, Des Rosier KF, Charlesworth RW,Jr. Quantitative measurement of erosion growth and joint space loss in rheumatoid arthritis hand radiographs. J Rheumatol. 1996 Feb;23(2):265-72.

72. Sharp JT, Angwin J, Boers M, Duryea J, von Ingersleben G, Hall JR, et al. Computer based methods for measurement of joint space width: Update of an ongoing OMERACT project. J Rheumatol. 2007 Apr;34(4):874-83.

73. Lukas C, Sharp JT, Angwin J, Boers M, Duryea J, Hall JR, et al. Automated measurement of joint space width in small joints of patients with rheumatoid arthritis. J Rheumatol. 2008 Jul;35(7):1288-93.

74. Duryea J, Dobbins JT,3rd, Lynch JA. Digital tomosynthesis of hand joints for arthritis assessment. Med Phys. 2003 Mar;30(3):325-33.

75. Finckh A, de Pablo P, Katz JN, Neumann G, Lu Y, Wolfe F, et al. Performance of an automated computer-based scoring method to assess joint space narrowing in rheumatoid arthritis: A longitudinal study. Arthritis Rheum. 2006 May;54(5):1444-50.

76. Langs G, Peloschek P, Bischof H, Kainberger F. Automatic quantification of joint space narrowing and erosions in rheumatoid arthritis. IEEE Trans Med Imaging. 2009 Jan;28(1):151-64.

77. Sharp JT, Gardner JC, Bennett EM. Computer-based methods for measuring joint space and estimating erosion volume in the finger and wrist joints of patients with rheumatoid arthritis. Arthritis Rheum. 2000 Jun;43(6):1378-86.

78. Angwin J, Heald G, Lloyd A, Howland K, Davy M, James MF. Reliability and sensitivity of joint space measurements in hand radiographs using computerized image analysis. J Rheumatol. 2001 Aug;28(8):1825-36.

79. Angwin J, Lloyd A, Heald G, Nepom G, Binks M, James MF. Radiographic hand joint space width assessed by computer is a sensitive measure of change in early rheumatoid arthritis. J Rheumatol. 2004 Jun;31(6):1050-61.

80. James MF, Heald G, Shorter JH, Turner RA. Joint space measurement in hand radiographs using computerized image analysis. Arthritis Rheum. 1995 Jul;38(7):891-901.

81. Kauffman JA, Slump CH, Moens HJB. In: Segmentation of hand radiographs with multilevel connected active appearance models. Medical imaging: Image processing 2005;5747-82. Proceedings of SPIE.

82. Kauffman JA, Slump CH, Moens HJB. In: Detection of joint space narrowing in hand radiographs. Medical imaging: Image processing 2006;6144-149. Proceedings of SPIE.

83. McQueen F, Ostergaard M, Peterfy C, Lassere M, Ejbjerg B, Bird P, et al. Pitfalls in scoring MR images of rheumatoid arthritis wrist and metacarpophalangeal joints. Ann Rheum Dis. 2005 Feb;64 Suppl 1:i48-55.

84. McQueen F, Clarke A, McHaffie A, Reeves Q, Williams M, Robinson E, et al. Assessment of cartilage loss at the wrist in rheumatoid arthritis using a new MRI scoring system. Ann Rheum Dis. 2010 Nov;69(11):1971-5.

85. Buckland-Wright JC, Carmichael I, Walker SR. Quantitative microfocal radiography accurately detects joint changes in rheumatoid arthritis. Ann Rheum Dis. 1986 May;45(5):379-83.

86. Duryea J, Magalnick M, Alli S, Yao L, Wilson M, Goldbach-Mansky R. Semiautomated three-dimensional segmentation software to quantify carpal bone volume changes on wrist CT scans for arthritis assessment. Med Phys. 2008 Jun;35(6):2321-30.

87. Ostergaard M, Peterfy C, Conaghan P, McQueen F, Bird P, Ejbjerg B, et al. OMERACT rheumatoid arthritis magnetic resonance imaging studies. Core set of MRI acquisitions, joint pathology definitions, and the OMERACT RA-MRI scoring system. J Rheumatol. 2003 Jun;30(6):1385-6.

88. McQueen F, Lassere M, Edmonds J, Conaghan P, Peterfy C, Bird P, et al. OMERACT rheumatoid arthritis magnetic resonance imaging studies. Summary of OMERACT 6 MR imaging module. J Rheumatol. 2003 Jun;30(6):1387-92.

89. Bird P, Lassere M, Shnier R, Edmonds J. Computerized measurement of magnetic resonance imaging erosion volumes in patients with rheumatoid arthritis: A comparison with existing magnetic resonance imaging scoring systems and standard clinical outcome measures. Arthritis Rheum. 2003 Mar;48(3):614-24.

90. Bird P, Joshua F, Lassere M, Shnier R, Edmonds J. Training and calibration improve inter-reader reliability of joint damage assessment using magnetic resonance image scoring and computerized erosion volume measurement. J Rheumatol. 2005 Aug;32(8):1452-8.

91. Bottcher J, Pfeil A. Diagnosis of periarticular osteoporosis in rheumatoid arthritis using digital X-ray radiogrammetry. Arthritis Res Ther. 2008;10(1):103.

92. Jensen T, Klarlund M, Hansen M, Jensen KE, Podenphant J, Hansen TM, et al. Bone loss in unclassified polyarthritis and early rheumatoid arthritis is better detected by digital x ray radiogrammetry than dual x ray absorptiometry: Relationship with disease activity and radiographic outcome. Ann Rheum Dis. 2004 Jan;63(1):15-22.

93. Jensen T, Hansen M, Jensen KE, Podenphant J, Hansen TM, Hyldstrup L. Comparison of dual X-ray absorptiometry (DXA), digital X-ray radiogrammetry (DXR), and conventional radiographs in the evaluation of osteoporosis and bone erosions in patients with rheumatoid arthritis. Scand J Rheumatol. 2005;34(1):27-33.

94. Alenfeld FE, Diessel E, Brezger M, Sieper J, Felsenberg D, Braun J. Detailed analyses of periarticular osteoporosis in rheumatoid arthritis. Osteoporos Int. 2000;11(5):400-7.

95. Harrison BJ, Hutchinson CE, Adams J, Bruce IN, Herrick AL. Assessing periarticular bone mineral density in patients with early psoriatic arthritis or rheumatoid arthritis. Ann Rheum Dis. 2002 Nov;61(11):1007-11.

96. Fleming A, Crown JM, Corbett M. Incidence of joint involvement in early rheumatoid arthritis. Rheumatol Rehabil. 1976 May;15(2):92-6.

97. Mattingly PC, Matheson JA, Dickson RA. The distribution of radiological joint damage in the rheumatoid hand. Rheumatol Rehabil. 1979 Aug;18(3):142-7.

98. Owsianik WD, Kundi A, Whitehead JN, Kraag GR, Goldsmith C. Radiological articular involvement in the dominant hand in rheumatoid arthritis. Ann Rheum Dis. 1980 Oct;39(5):508-10.

99. Krug R, Burghardt AJ, Majumdar S, Link TM. High-resolution imaging techniques for the assessment of osteoporosis. Radiol Clin North Am. 2010 May;48(3):601-21.

100. [Internet]. Available from: www.scanco.ch.

101. MacNeil JA, Boyd SK. Improved reproducibility of high-resolution peripheral quantitative computed tomography for measurement of bone quality. Med Eng Phys. 2008 Jul;30(6):792-9.

102. MacNeil JA, Boyd SK. Accuracy of high-resolution peripheral quantitative computed tomography for measurement of bone quality. Med Eng Phys. 2007 Dec;29(10):1096-105.

103. Macdonald HM, Nishiyama KK, Kang J, Hanley DA, Boyd SK. Age-related patterns of trabecular and cortical bone loss differ between sexes and skeletal sites: A population-based HR-pQCT study. J Bone Miner Res. 2011 Jan;26(1):50-62.

104. Macneil JA, Boyd SK. Bone strength at the distal radius can be estimated from high-resolution peripheral quantitative computed tomography and the finite element method. Bone. 2008 Jun;42(6):1203-13.

105. MacNeil JA, Boyd SK. Accuracy of high-resolution peripheral quantitative computed tomography for measurement of bone quality. Med Eng Phys. 2007 Dec;29(10):1096-105.

106. Stach CM, Bauerle M, Englbrecht M, Kronke G, Engelke K, Manger B, et al. Periarticular bone structure in rheumatoid arthritis patients and healthy individuals

assessed by high-resolution computed tomography. Arthritis Rheum. 2010 Feb;62(2):330-9.

107. Finzel S, Englbrecht M, Engelke K, Stach C, Schett G. A comparative study of periarticular bone lesions in rheumatoid arthritis and psoriatic arthritis. Ann Rheum Dis. 2011 Jan;70(1):122-7.

108. Finzel S, Ohrndorf S, Englbrecht M, Stach C, Messerschmidt J, Schett G, et al. A detailed comparative study of high-resolution ultrasound and micro-computed tomography for detection of arthritic bone erosions. Arthritis Rheum. 2011 May;63(5):1231-6.

109. Fouque-Aubert A, Boutroy S, Marotte H, Vilayphiou N, Bacchetta J, Miossec P, et al. Assessment of hand bone loss in rheumatoid arthritis by high-resolution peripheral quantitative CT. Ann Rheum Dis. 2010 Sep;69(9):1671-6.

110. Arnett FC, Edworthy SM, Bloch DA, McShane DJ, Fries JF, Cooper NS, et al. The American Rheumatism Association 1987 revised criteria for the classification of rheumatoid arthritis. Arthritis Rheum. 1988 Mar;31(3):315-24.

111. Buie HR, Campbell GM, Klinck RJ, MacNeil JA, Boyd SK. Automatic segmentation of cortical and trabecular compartments based on a dual threshold technique for in vivo micro-CT bone analysis. Bone. 2007 Oct;41(4):505-15.

112. Hildebrand T, Ruegsegger P. A new method for the model-independent assessment of thickness in three-dimensional images. Journal of Microscopy. 1997;185:67-75.

113. Bland M. How should I calculate a within-subject coefficient of variation? [Internet].; 2006 [updated 16 October, 2006. Available from: http://www-users.york.ac.uk/~mb55/meas/cv.htm.

114. Viera AJ, Garrett JM. Understanding interobserver agreement: The kappa statistic. Fam Med. 2005 May;37(5):360-3.

115. Soreide K, Korner H, Soreide JA. Diagnostic accuracy and receiver-operating characteristics curve analysis in surgical research and decision making. Ann Surg. 2011 Jan;253(1):27-34.

116. Kolling C, Stok KS, Mueller TL, Muller R, Goldhahn J. In vivo microstructural quantification of finger joints using high-resolution pQCT. American Society for Bone and Mineral Research 2010 Annual Meeting. 2010.

117. Haavardsholm EA, Ostergaard M, Ejbjerg BJ, Kvan NP, Uhlig TA, Lilleas FG, et al. Reliability and sensitivity to change of the OMERACT rheumatoid arthritis magnetic resonance imaging score in a multireader, longitudinal setting. Arthritis Rheum. 2005 Dec;52(12):3860-7.

118. van der Heijde DM. Plain X-rays in rheumatoid arthritis: Overview of scoring methods, their reliability and applicability. Baillieres Clin Rheumatol. 1996 Aug;10(3):435-53.

119. Aletaha D, Funovits J, Smolen JS. Extended report: Physical disability in rheumatoid arthritis is associated with cartilage damage rather than bone destruction. Ann Rheum Dis. 2011 May;70(5):733-9.

120. Pfeil A, Haugeberg G, Hansch A, Renz DM, Lehmann G, Malich A, et al. Value of digital X-ray radiogrammetry in the assessment of inflammatory bone loss in rheumatoid arthritis. Arthritis Care Res (Hoboken). 2011 May;63(5):666-74.